PHYSICAL REVIEW B VOLUME 41, NUMBER 7 1 MARCH 1990

# Extension of the random-phase-approximation theory of ferromagnetism in a magnetic field applicable at all temperatures

A. Czachor
*Institute of Physics of the Polish Academy of Sciences, Lotnikow 32/46, 02-668 Warsaw, Poland*

A. Holas
*Institute of Physical Chemistry of the Polish Academy of Sciences, Kasprzaka 44, 01-224 Warsaw, Poland*
(Received 19 June 1989)

Generalization of the random-phase-approximation (RPA) theory of ferromagnetism for spins $S=\frac{1}{2}$, based on a refinement of the decoupling for a relevant three-spin Green's function, is presented. With the reasonable choice of two characteristic functions of the present theory—the virtual spectrum $\Delta(\omega)$ and the decoupling factor $\kappa(\sigma)$, where $\omega$ is an excitation energy and $\sigma$ is the relative magnetization—the theory provides a fair description of magnetic phenomena not only at temperature $T\rightarrow 0$, in the vicinity of the Curie temperature $T_C$, or at high $T$, but at all temperatures and external magnetic fields $H$. A relation between some parameters of the functions $\Delta(\omega)$ and $\kappa(\sigma)$, and the critical indices of the static scaling theory, has been established. The form of the universal scaling function $W$, following from our theory, has been found. For the power-law virtual spectrum $\Delta \propto \omega^s$ at $\omega \rightarrow 0$, $0<s<1$, we have found the nonanalytic increase of the magnetization versus the field at $T<T_C$: $\sigma(T,H)-\sigma(T,0)\propto H^s$. It reduces to the classic result of Holstein and Primakoff for the three-dimensional isotropic Heisenberg ferromagnet having $s=\frac{1}{2}$. Assuming this power-law spectrum at all energies up to some cutoff energy, we have obtained a rather good agreement of the present predictions for $\sigma(T,H)$ with experimental data for Ni, for all temperatures and fields available. Some model virtual spectra are found to lead to interesting models of ferromagnetism, with the magnetization and the susceptibility functions given in terms of explicit analytic formulas.

## I. INTRODUCTION

The spin-wave theory for the isotropic Heisenberg ferromagnet in three dimensions (3DIH) predicts that close to the temperature $T=0$ the magnetization $M(T,H)$ grows with the small magnetic field $H$ as $\delta M = M(T,H)-M(T,0)\propto H^{1/2}$, see Holstein and Primakoff.[1] Near the Curie temperature $T_C$ the static scaling hypothesis is generally considered to be valid,[2] and one speaks of magnetic phenomena in terms of linear susceptibility $\chi$ and critical indices $\beta$, $\Delta$, $\gamma$, and $\gamma'$. Rather naturally, there arises the question, whether, and in which way, the predictions of both approaches match at intermediate temperatures. Some authors could have been aware of this problem (see Ref. 2, p. 20), but so far it has not been analyzed openly, it seems.

The system of localized spins $S=\frac{1}{2}$ coupled ferromagnetically is a prototype of real ferromagnetic systems, and its properties have been analyzed in many approximations.[3-11] The quantum-mechanical aspect of the spin dynamics is strong here, but fortunately the equations of motion for the spin operators are relatively simple. This allows one to describe many properties of such systems analytically, at least in the random-phase approximation (RPA), as has been done by Bogolyubov and Tyablikov.[3,4] Somehow, the physical content of this important work has been little investigated, and, for example, the behavior of $\delta M$ versus $H$ for $H\rightarrow 0$ in the RPA has not been known, although numerical analysis of Flax[11] at finite $H$ suggested a nonlinear behavior in this limit.

The aim of this paper is twofold: (i) to generalize the RPA theory so that it allows us a fair interpolation between the spin-wave $T\rightarrow 0$ region and the static scaling $T\rightarrow T_c$ region and (ii) to predict the analytical behavior of the relative magnetization $\sigma$ and the initial susceptibility $\chi$ in the generalized RPA (its label is MCRPA, to be explained later) and the RPA itself, at all limits of interest in the whole $T$-$H$ plane. Besides, we demonstrate that this theoretical scheme is rather versatile and can be specified to generate a number of interesting models of ferromagnetism.

The plan of this paper is as follows: In Sec. II we introduce a correction of the RPA decoupling of the relevant three-spin Green's function (GF), which results in the aforementioned generalization of the RPA—the MCRPA. In Sec. III a basic equation of state relating $\sigma$, $T$, and $H$, and an equation relating $\chi$ and $T$ are derived, and a comparison with some exact results is done; here a useful notion of the "virtual spectrum," related to the spectrum of elementary magnetic excitations, is introduced. For some model virtual spectra we solve the MCRPA equations analytically—see Sec. IV. The leading term of the field dependence of the magnetization below $T_C$ has been established in Sec. V. In Sec. VI we give a rather full analysis of the $T$ and $H$ dependence of the magnetization at $T\rightarrow 0$, and determine conditions for some spurious terms to vanish. An equation of state near $T_C$ has been derived in Sec. VII and Appendix E; in Sec.

 

VIII it has been rewritten in the form of the scaling equation, with critical indices given in terms of formal parameters $s,p$ of the present theory (related to the virtual spectrum and a decoupling factor, respectively). Some MCRPA models of ferromagnetism have been numerically analyzed in Sec. IX. Then in Sec. X we show that, in spite of a rather simplistic choice of the virtual spectrum, the present approach allows us a good fit of its predictions with experimental data for nickel. A summary of conclusions is given in Sec. XI.

In the main body of this paper we mainly present a simple intuitive argument. As such an analysis has not been done so far even for the RPA, a rather full treatment, including derivations and mathematical details, has been given in the Appendixes.

## II. A CORRECTION OF THE RPA DECOUPLING

Let us consider an anisotropic Heisenberg ferromagnet in an external magnetic field $H$ directed along its anisotropy axis (chosen to be the $z$ axis). The Hamiltonian of such a system of $N$ spins $S=\frac{1}{2}$ is

$$\mathcal{H}=-\frac{1}{2}\sum_{\substack{l,l'\\ l\neq l'}}[J^{\parallel}_{l-l'}S^z_lS^z_{l'}+J^{\perp}_{l-l'}(S^x_lS^x_{l'}+S^y_lS^y_{l'})]-\mu H\sum_l S^z_l , \tag{2.1}$$

where $\mu$ is the product of the Lande factor and the Bohr magneton. With the coupling constants $J^{\perp}_l=0$ and $J^{\parallel}_l>0$ it is the Ising ferromagnet, whereas for $J^{\parallel}_l=J^{\perp}_l>0$ we have the isotropic ferromagnet. We shall consider some intermediate anisotropic cases too. $S^x_l$, $S^y_l$, and $S^z_l$ are the usual spin operators attached to the lattice site $l$.

In this work we shall follow the derivations of Bogolyubov and Tyablikov[3,4] (BT), and Plakida.[5] It is convenient to introduce the relative magnetization

$$\sigma=\langle S^z_l\rangle_T/S . \tag{2.2}$$

Actually, because of the lattice translational invariance of the system, $\sigma$ is independent of the lattice vector $l$. Here $\langle X\rangle_T$ is the thermal average of the operator $X$ with the Hamiltonian (2.1). We recall that for $S=\frac{1}{2}$ the following relation holds:

$$S^z_l=\tfrac{1}{2}-S^-_lS^+_l , \tag{2.3}$$

where $S^{\pm}=S^x\pm iS^y$. Therefore, the magnetization we seek can be expressed in terms of the correlation function $\langle S^-S^+\rangle_T$, which can be determined, via the spectral theorem,[4] from the corresponding double-time Green's function (GF). Using the equation $i\dot{X}=[X,\mathcal{H}]$, we obtain for this GF,

$$G_{l-l'}(t-t')\equiv\langle\langle S^+_l(t),S^-_{l'}(t')\rangle\rangle = -i\Theta(t-t')\langle[S^+_l(t),S^-_{l'}(t')]\rangle_T , \tag{2.4}$$

the following equation of motion:

$$\left[\frac{id}{dt}-\mu H\right]G_{l-l'}(t-t')=\delta(t-t')\langle[S^+_l,S^-_{l'}]\rangle_T+\sum_{l''\neq l'}[J^{\parallel}_{l-l''}\langle\langle S^z_{l''}(t)S^+_l(t),S^-_{l'}(t')\rangle\rangle-J^{\perp}_{l-l''}\langle\langle S^z_l(t)S^+_{l''}(t),S^-_{l'}(t')\rangle\rangle] , \tag{2.5}$$

where $[X,Y]$ stands for the commutator of $X$ and $Y$, and $t$ is time.

The two-spin GF on the left-hand side (LHS) of Eq. (2.5) depends on a three-spin GF on the right-hand side (RHS). A general strategy of the Green's-function methods in such cases is to approximate the three-spin GF by an appropriate combination of two-spin GF's. Several ingenious "decoupling" schemes have been developed; let us just quote Callen,[6] Katsura and Horigushi,[7] and Kumar and Gupta,[8] and the references quoted there. An interesting comparison of relative merits of the commutator and the anticommutator Green's functions has been made by Schreiber.[9]

These studies, usually aimed at the low-temperature expansions of the magnetization at $H=0$, provide a description that is rather complex and therefore not too convenient for predicting the magnetization at nonzero fields and at elevated temperatures. Instead, in this paper we propose an extension of the BT treatment, which retains its formal structure and yet allows us to interpolate approximately between the low-temperature Bloch-type behavior of the magnetization and the static-scaling (or renormalization-group) dominated behavior near the Curie temperature.

Let us generalize the BT decoupling (also called the random-phase approximation, RPA, in this context), on requesting that

$$\langle\langle S^z_l(t)S^+_{l''}(t),S^-_{l'}(t')\rangle\rangle\simeq\kappa_{ll'l''}\langle S^z_l\rangle_T\langle\langle S^+_{l''}(t),S^-_{l'}(t')\rangle\rangle . \tag{2.6}$$

As follows from Eq. (2.5), we need it for $l''\neq l$ only. On setting $\kappa_{ll'l''}=1$, we return to the BT decoupling, leading to the $T^{3/2}$ behavior of the magnetization at $T\to 0$, and to the critical index $\beta=\frac{1}{2}$ near the Curie temperature $T_C$. Instead of following the RPA, let us try to gain some insight into the nature of the decoupling factor $\kappa_{ll'l''}$, via the simplest integral characteristic of the GF's involved: We request that leading frequency moments of both sides of Eq. (2.6) should be equal. Taking into account that for the GF of the $\langle\langle X(t),Y(t')\rangle\rangle$ type the zeroth moment is $\langle[X,Y]\rangle_T$, we arrive at the equation

$$2\langle S^z_lS^z_{l''}\rangle_T\delta_{l'l''}-\langle S^-_{l'}S^+_{l''}\rangle_T\delta_{ll'}\simeq 2\kappa_{ll'l''}\langle S^z\rangle^2_T\delta_{l'l''} . \tag{2.7}$$

Although for some combinations of indices the equality of both sides turns out to be impossible, in the important case $l'=l''\neq l$ we obtain from (2.7)

$$\kappa_{ll'l''}\simeq\langle S^z_lS^z_{l'}\rangle_T/\langle S^z\rangle^2_T . \tag{2.8}$$

Intuitively, this form looks natural. The two-spin correlation function appears here in the decoupling procedure, which is in the spirit of the Callen concept.[6] Note that the decoupling factor (2.8) goes to unity when $T \to 0$ because in the ground state all spins should be parallel.

We want to introduce, via the decoupling factor, more realistic information about the three-spin correlation than is in the RPA, without changing substantially the formal structure of the RPA. Therefore, in the following we drop all subscripts, assuming $\kappa$ to be the same for all combinations of $l, l', l'$, appearing in the calculations. Equation (2.8) suggests that the $\sigma$ dependence of $\kappa$ should be crucial. Therefore, it is postulated here that $\kappa$ depends on $T$ and $H$ via $\sigma(T,H)$ only. The form of the function $\kappa(\sigma)$ will be specified later.

Let us mention that in terms of the more general decoupling scheme proposed recently by Kumar and Gupta[8] our decoupling is a special case, corresponding to the following decoupling factors of them:

$$f_1 = (1-\sigma\kappa)/(1-\sigma), \; f_2 = f_3 = 0 \; .$$

As $\kappa$ is just a number, not an operator, further steps of the BT derivation remain the same, and we end up with the RPA-type equation,[3–5]

$$\sigma = \left[ \frac{1}{N} \sum_{\mathbf{q} \in \mathrm{BZ}} \coth \left[ \frac{E_{\mathbf{q}}}{2T} \right] \right]^{-1} . \tag{2.9}$$

Now, however, the magnetic excitation energy depends also on $\kappa(\sigma)$,

$$E_{\mathbf{q}} = \mu H + \sigma \kappa(\sigma) \omega_{\mathbf{q}} \; . \tag{2.10}$$

Temperature and frequency are taken in units of energy, $k_B T \to T$ and $\hbar\omega \to \omega$, here and throughout the paper. The wave vector $\mathbf{q}$ belongs to the first Brillouin zone (BZ) and $\omega_{\mathbf{q}}$ is defined as follows:

$$\omega_{\mathbf{q}} = \tfrac{1}{2} \sum_{l \neq 0} [J_l^{\parallel} - J_l^{\perp} \exp(i\mathbf{q}\cdot\mathbf{l})] \; . \tag{2.11}$$

According to Eq. (2.10), we can treat $\omega_{\mathbf{q}}$ as the excitation energy per unit magnetization [to be precise, per unit of the product $\sigma\kappa(\sigma)$], in the limit $H \to 0$, say, a virtual excitation energy. Note that the self-consistency enters into Eq. (2.9) not only through the factor $\sigma$ (as in RPA) but also through the decoupling factor $\kappa(\sigma)$ in Eq. (2.10).

## III. FORMULATION OF THE THEORY IN TERMS OF VIRTUAL SPECTRUM. HIGH-$T$ EXPANSION OF THE SUSCEPTIBILITY

In further sections of this paper we shall investigate the physical content of Eqs. (2.9) and (2.10) under some assumptions concerning the form of $\kappa(\sigma)$. As the very possibility of introducing the $\kappa$ different from unity and $\sigma$ dependent has appeared to us via the analysis of moments of relevant Green's functions, we shall call this approach the "moment corrected" RPA theory (MCRPA), just to distinguish it from other theories related to the RPA.

It turns out that even in the classic RPA case ($\kappa = 1$) these formulas so far have not been analyzed with the care they deserve. To pursue this aim, we have found it very useful to introduce the notion of an auxiliary spectrum $\Delta(\omega)$. First, let us recall the notion of the spectrum of energies $E_{\mathbf{q}}$ of elementary excitations, i.e., the density of states

$$g(\omega) = N^{-1} \sum_{\mathbf{q} \in \mathrm{BZ}} \delta(\omega - E_{\mathbf{q}}), \; \int d\omega \, g(\omega) = 1 \; . \tag{3.1}$$

Clearly, this spectrum depends on the "external" parameters $T, H$.

Explicit considerations of the details of the $\mathbf{q}$ dependence in (2.11) and of the $\mathbf{q}$ integration in (2.9) can be difficult. To avoid it, let us introduce the "density of virtual states," or the "virtual spectrum"

$$\Delta(\omega) = N^{-1} \sum_{\mathbf{q} \in \mathrm{BZ}} \delta(\omega - \omega_{\mathbf{q}}), \; \int d\omega \, \Delta(\omega) = 1 \; . \tag{3.2}$$

This function is an inner characteristic of the system, depending only on the material constants, $J_l^{\parallel}$ and $J_l^{\perp}$, and on the crystal structure, given by the lattice vectors $\mathbf{l}$. It is related to the spectrum of elementary excitations (3.1) by the obvious relation

$$g(\omega) = \Delta([\omega - \mu H]/[\sigma\kappa(\sigma)])/[\sigma\kappa(\sigma)] \; . \tag{3.3}$$

An analysis of the low-frequency behavior of $\Delta(\omega)$ for an isotropic Heisenberg model (to be used later to explore the low-$T$ and low-$H$ magnetization in the MCRPA) is given in Appendix A.

Using the virtual spectrum, we can rewrite Eq. (2.9)—the equation of state for this system—in the following form:

$$\sigma = \left[ \left\langle \coth \left[ \frac{\mu H + \sigma\kappa(\sigma)\omega}{2T} \right] \right\rangle \right]^{-1} . \tag{3.4a}$$

Here we have introduced the notation for an average with $\Delta(\omega)$,

$$\langle f(\omega) \rangle \equiv \int d\omega \, \Delta(\omega) f(\omega) \; , \tag{3.4b}$$

to be used from now on. Let us note here that the well-known relation for the magnetization, $\sigma(T,-H) = -\sigma(T,H)$, results, via (3.4a), in a relation for the decoupling factor

$$\kappa(-\sigma) = \kappa(\sigma) \; . \tag{3.5}$$

The form (3.4) of the equation of state, being equivalent to the original Eq. (2.9), is more convenient than (2.9) because it involves only one-dimensional integration. It offers a perspective of study models characterized by various virtual spectra, and an opportunity to derive a number of special cases and to sysematize them without any explicit reference to dispersion relations of magnetic excitations or to dimensionality or symmetry of the system investigated. In particular, it allows one to examine models characterized by the virtual spectra of the origin different from the Heisenberg Hamiltonian (2.1).

In other words, the magnetization in the MCRPA, as expressed by Eq. (3.4), is a functional of two functions: $\Delta(\omega)$ and $\kappa(\sigma)$.

In the following we shall not return too often to the roots of this equation. Rather, we shall rely on a general phenomenological argument in accepting a reasonable form of both functions to examine the variety of magnetic phenomena following from the MCRPA.

To demonstrate the first advantage of the approach proposed, let us look at the Curie temperature $T_C$. Putting $H=0$ and $\sigma \to 0$ in (3.4) we find

$$T_C = \frac{1}{2\langle \omega^{-1} \rangle} \lim_{\sigma \to 0} \kappa(\sigma) \equiv \frac{\kappa_0}{2\langle \omega^{-1} \rangle} . \tag{3.6}$$

This shows that the critical behavior of magnetization is, within the MCRPA, crucially sensitive to the form of $\Delta(\omega)$ in the vicinity of $\omega=0$. With $\kappa_0$ finite and positive the system can be ferromagnetic only if $\langle \omega^{-1} \rangle$ is finite and nonzero.

Another important characteristic of ferromagnets, besides the magnetization

$$M(T,H) = \mu S \sigma(T,H) , \tag{3.7}$$

is the so-called "initial susceptibility" $\chi(T)$, or its inverse $r(T)$, defined as follows for $S=\frac{1}{2}$:

$$\chi(T) = \lim_{H \to 0} \frac{\partial M(T,H)}{\partial H} = \frac{\mu^2}{2} \lim_{H \to 0} \frac{\partial \sigma(T,H)}{\partial(\mu H)} , \tag{3.8}$$

$$r(T) = \frac{\mu^2}{2\chi(T)} \tag{3.9}$$

[note that $r(T)$ is in units of energy]. Using Eq. (3.4), we can easily derive a relation between the susceptibility and the temperature for the paramagnetic region, $T > T_C$. In order to do this, we replace the $\sigma$ on both sides of Eq. (3.4a) by its small-$H$ expansion

$$\sigma(T,H) = \sigma(T,0) + \frac{\partial \sigma}{\partial H} H + O(H^2) = 0 + \frac{\mu H}{r} + O(H^2) \tag{3.10}$$

and then take the limit $H \to 0$ to obtain

$$\frac{1}{2T} = \int \frac{\Delta(\omega)}{r + \kappa_0 \omega} d\omega . \tag{3.11}$$

This elegant equation shows that to determine the relation between $r$ and $T$ in the MCRPA it is enough to find the Hilbert transform of the virtual spectrum $\Delta(\omega)$. The high-$T$ expansion of $r(T)$ obtained from this equation is as follows:

$$\frac{2T}{r} = \frac{4T\chi(T)}{\mu^2} = 1 + \langle \omega \rangle \frac{\kappa_0}{2T} + (2\langle \omega \rangle^2 - \langle \omega^2 \rangle) \left[ \frac{\kappa_0}{2T} \right]^2 + O\left( \left[ \frac{\langle \omega \rangle}{2T} \right]^3 \right) , \tag{3.12}$$

where the moments can be easily calculated. For this isotropic coupling, $J_l^{\parallel} = J_l^{\perp} = J_l$, we have

$$\langle \omega \rangle = \tfrac{1}{2} \sum_l J_l , \tag{3.13}$$

$$\langle \omega^2 \rangle = \tfrac{1}{4} \sum_l J_l^2 + \left[ \tfrac{1}{2} \sum_l J_l \right]^2 . \tag{3.14}$$

Expansion (3.12) may be compared with the exact high-$T$ expansion obtained by perturbation methods (see, e.g., Tyablikov[4]) for cubic lattices, with the interspin coupling $J=I$ restricted to $z$ nearest neighbors,

$$\frac{4T\chi_{\text{pert}}(T)}{\mu^2} = 1 + \frac{zI}{4T} + \left[ 1 - \frac{2}{z} \right] \left[ \frac{zI}{4T} \right]^2 + O\left[ \left[ \frac{I}{T} \right]^3 \right] . \tag{3.15}$$

In such cases the moments (3.13) and (3.14) reduce to

$$\langle \omega \rangle = zI/2 , \tag{3.16}$$

$$\langle \omega^2 \rangle = (1 + 1/z) \langle \omega \rangle^2 . \tag{3.17}$$

Thus, in order to have the leading terms of the MCRPA expansion (3.12) the same as in the exact expansion (3.15), we must assume

$$\kappa_0 \equiv \kappa(0) = 1 . \tag{3.18}$$

If we choose this value for $\kappa_0$, the $\chi(T)$ of the MCRPA becomes the same as the one of the RPA. The discrepancy between the RPA and the exact result starts from the next term,

$$\frac{4T}{\mu^2} [\chi_{\text{RPA}}(T) - \chi_{\text{pert}}(T)] = \frac{1}{z} \left[ \frac{zI}{4T} \right]^2 + O\left[ \left[ \frac{zI}{4T} \right]^3 \right] . \tag{3.19}$$

It is noteworthy that this discrepancy might be removed by a modification of the virtual spectrum, such that $\langle \omega^2 \rangle$ of Eq. (3.17) is replaced by

$$\langle \omega^2 \rangle_{\text{pert}} = (1 + 2/z) \langle \omega \rangle^2 . \tag{3.20}$$

Similarly, by an appropriate modification of higher moments, we might correct the higher-order terms of (3.12).

Having established the conditions of reconciliation between the present approach and the exact results, we find out that they are too restrictive if we are interested in a single simple scheme capable of describing the experimental situation fairly at all temperatures and fields. This is why in the next sections we shall turn a blind eye to the condition $\kappa_0 = 1$. Hopefully, a more consequent treatment of this point will emerge in the future.

On comparing Eq. (3.11) with (3.6) we see that $r \to 0$ when $T \to T_C + 0^+$. Let us recall that according to the static-scaling theory[2] the $r(T)$ should have at this limit a power-law character

$$r(T) \propto \chi^{-1} \propto (T - T_C)^{\gamma} . \tag{3.21}$$

This relation defines the critical index $\gamma$; a similar relation holds for the critical $\gamma'$ in the region $T < T_C$,

$$r(T) \propto \chi^{-1} \propto (T_C - T)^{\gamma'} , \tag{3.22}$$

provided that $r$ is finite in this region.

## IV. FULLY SOLUBLE MCRPA MODELS

Let us stress here the point of view (to be proven in further sections) that the moment-corrected RPA is not only a useful theory of ferromagnetism, allowing one to interpret and understand, at least semiquantitatively, several subtle phenomena. Also, especially in the virtual spectrum formulation (3.4), it leads to simple but nontrivial models of ferromagnetism, showing merits of clarity and transparency. In this sense, the present work gives an integration of the theory of ferromagnetism at a level of reasonable precision reconciled with relative simplicity.

As a good entry point, we shall present in this section some simple, fully soluble models. For the Ising case, $J_l^{\perp}=0$, there is only one excitation energy $\omega_I$, and we have

$$\Delta(\omega)=\delta(\omega-\omega_I) , \tag{4.1}$$

where

$$\omega_I=\sum_{l\neq 0} J_l^{\parallel} . \tag{4.2}$$

Using (3.4), we immediately obtain the molecular-(internal- or mean-) field, Weiss-type equation

$$\sigma=\tanh\left[\frac{\mu H+\sigma\kappa(\sigma)\omega_I}{2T}\right] , \tag{4.3}$$

and from (3.11) for the paramagnetic inverse susceptibility,

$$r(T)=2(T-T_C),\quad T_C=\kappa_0\omega_I/2 . \tag{4.4}$$

In particular, with the RPA decoupling factor $\kappa=1$, one has just the Weiss equation. Such a derivation of this textbook formula shows an interrelation between the Weiss and the Ising concepts, and suggests possible extensions of them.

For the intermediate case $J_l^{\parallel}>J_l^{\perp}>0$ the virtual spectrum is broad and shows a gap at low energies. As a rough imitation of such a situation, we can take the rectangular (uniform) spectrum

$$\Delta(\omega)=\Theta((B-\omega)(\omega-A))/(B-A),\quad B>A>0 . \tag{4.5}$$

From (3.6) we immediately get the corresponding Curie temperature

$$T_C=\frac{(B-A)\kappa_0}{2\ln(B/A)} \tag{4.6}$$

and from (3.4) the form of the equation of state for this case,

$$\sinh\left[\frac{\mu H+\sigma\kappa(\sigma)B}{2T}\right]=\exp\left[\frac{\kappa(\sigma)(B-A)}{2T}\right]\times\sinh\left[\frac{\mu H+\sigma\kappa(\sigma)A}{2T}\right] . \tag{4.7}$$

The initial inverse susceptibility for $T>T_C$ follows easily from Eq. (3.11). In terms of the scaled reciprocal temperature $\tau=T_C/T$ and $C=B/A$ we have

$$r(T)=2T_C\frac{C\ln C}{C-1}\frac{1-C^{\tau-1}}{C^{\tau}-1} . \tag{4.8}$$

Close to $T_C$ it is

$$r(T)=2C\left[\frac{\ln C}{C-1}\right]^2(T-T_C)+O((T-T_C)^2) , \tag{4.9}$$

i.e., the critical index [see Eq. (3.21)] is $\gamma=1$. Similar expansion below $T_C$ follows directly from Eqs. (3.9), (3.8), and (4.7). To avoid at this stage, a discussion of the $\sigma$ dependence of $\kappa$ near $T_C$, let us write the formula for the RPA case $\kappa=1$,

$$r(T)=4C\left[\frac{\ln C}{C-1}\right]^2(T_C-T)+O((T_C-T)^2) . \tag{4.10}$$

We can see that the corresponding critical exponent $\gamma'$ is also 1. At the same time the coefficients multiplying $|T-T_C|$ differ by a factor of 2; the same occurs in the classic MFA; see Fisher's[2] comments to his Eq. (3.39).

For the RPA, with $C=2$, we have obtained from (4.7) the explicit formulas for the $T$ dependence of the spontaneous magnetization $\sigma(T,0)$ and the inverse susceptibility $r(T)$ for the whole ferromagnetic range of temperatures:

$$\sigma(T,0)=\log_2(2^{\tau-1}+(2^{2(\tau-1)}-1)^{1/2})/\tau , \tag{4.11}$$

$$r(T)=4T_C\ln(2)(2^{2(\tau-1)}-1),\quad \tau=T_C/T . \tag{4.12}$$

Similar explicit formulas can be obtained for $C=\frac{3}{2}$, 3, and 4.

The functions for $C=2$ have been shown in Fig. 1. As the formulas (4.8)–(4.12) are explicit and transparent, the rectangular-spectrum model is a particularly convenient model to demonstrate the basic features of ferromagnetic phenomena. Note that in the Weiss formula (4.3) the $\sigma$ versus $T$ dependence is given implicitly.

Interestingly, the Curie temperature (4.6) for the rectangular spectrum goes to zero when $A\to 0$. It is a hint that ferromagnetic ordering gets destroyed when the density of virtual states is too large at low energies. Note that such a situation, $\Delta(\omega)\to$const for $\omega\to 0$, corresponds to the two-dimensional isotropic Heisenberg system.

Examples of other model virtual spectra, leading to analytic solutions in the paramagnetic region $T>T_C$, are given in Appendix B and Table III. Interestingly, one finds here that the value of the critical index $\gamma$ depends on the presence or absence of a gap at $\omega=0$ in the virtual spectrum; see also Fig. 2. This point will be discussed later.

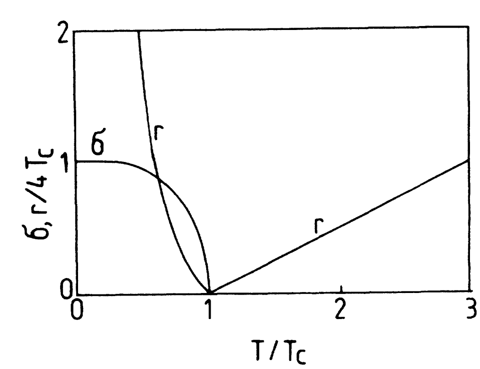


FIG. 1. The RPA (i.e., $\kappa=1$) spontaneous magnetization $\sigma(T,0)$, Eq. (4.11), and the scaled inverse magnetic susceptibility $r(T)/(4T_C)$, Eqs. (4.12) and (4.8), vs reduced temperature $T/T_C$, for the rectangular virtual spectrum (4.5) with $B/A=C=2$.

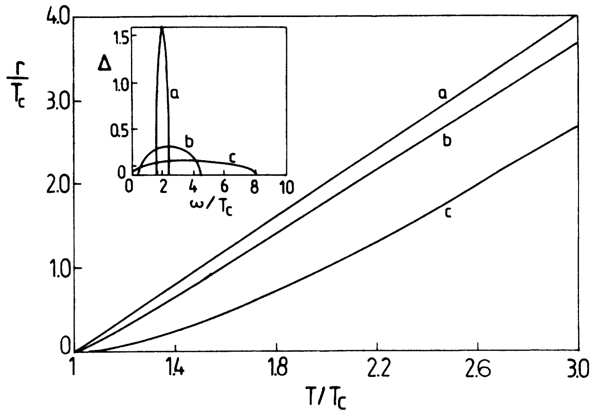


FIG. 2. The scaled inverse magnetic susceptibility $r(T)/T_C$ vs $T/T_C$ in the paramagnetic range of temperatures, $T>T_C$, in the RPA. The elliptic virtual spectrum (see Appendix B), shown in the inset, is chosen to mimic three different cases: (a) $\xi=4.0$—the spectrum close to $\delta(\omega-2T_C)$, which results in the classic mean-field behavior of the susceptibility [here $r\simeq2(T-T_C)$, i.e., the critical index $\gamma=1$], (b) $\xi=0.25$, a broad spectrum with a gap, $\gamma=1$, (c) $\xi=0.01$, (almost) gapless spectrum $\Delta\propto\omega^{1/2}$ for $\omega\to0$ (reminiscent of the spectrum for the 3D isotropic Heisenberg Hamiltonian at this limit). At $T\to T_C$ there is $r\propto(T-T_C)^2$, i.e., $\gamma=2$.

## V. FIELD DEPENDENCE OF MAGNETIZATION BELOW $T_C$

While there is a vast literature on the temperature dependence of the spontaneous magnetization, especially at $T\to0$ and $T\to T_C$, see the Introduction, its field dependence (except at $T_C$) seems to be an almost forgotten problem. We only have to mention here the numerical analysis for the $S=\frac{1}{2}$ isotropic Heisenberg ferromagnet in the RPA, done by Flax;[11] he has observed nonlinear trends in the $\sigma$ versus $H$ plots below $T_C$, but has not investigated the $H\to0$ limit. Even in the textbooks it is hard to find that in their classic paper Holstein and Primakoff have not only given their famous transformation, but have also proven for isotropic Heisenberg that at small $T$ the magnetization goes as

$$\delta\sigma=[\sigma(T,H)-\sigma(T,0)]\propto H^{1/2}$$

for $H\to0$. This means that the notion of initial susceptibility is not valid there. On the other hand, the static-scaling theory gives that at $T=T_C$ there is $\sigma\propto H^{1/\delta}$ for $H\to0$, and the scaling index $\delta$ is close to 5. In this section and Sec. VI we shall therefore investigate, what the predictions of the RPA and the MCRPA are for the intermediate range of temperatures, and whether one can use the present approach to interpolate between the temperature limits mentioned earlier.

First, on differentiating Eq. (3.4) with respect to $H$, taking the limit $H\to0$ and applying the definition (3.8), we obtain

$$\chi(T)=\sigma_0\mu^2\left\langle\left[\sinh\left(\frac{\sigma_0\kappa_0\omega}{2T}\right)\right]^{-2}\right\rangle\Big/[4T\Phi(\sigma_0,T)]\ , \tag{5.1}$$

where $\sigma_0=\sigma(T,0)$, the spontaneous magnetization, is a root of the equation

$$\varphi(\sigma,T)\equiv\sigma\left\langle\coth\left(\frac{\sigma\kappa(\sigma)\omega}{2T}\right)\right\rangle-1=0\ , \tag{5.2}$$

and

$$\Phi(\sigma_0,T)=\lim_{\sigma\to\sigma_0}\frac{\partial}{\partial\sigma}\varphi(\sigma,T)\ . \tag{5.3}$$

Obviously, $\Phi(\sigma_0,T)\neq0$ because $\sigma_0$ must be a single root of Eq. (5.2) in the range $0<T<T_C$. For the numerator of (5.1) to be finite, the necessary condition is that the integral

$$\langle\omega^{-2}\rangle\equiv\int_0^\infty d\omega\,\omega^{-2}\Delta(\omega) \tag{5.4}$$

must be convergent. Emergence appears at the lower limit of integration, unless there is a gap there in the virtual spectrum, as in the case with anisotropic interspin coupling, $J_l^{\parallel}>J_l^{\perp}$. However, for the isotropic Heisenberg ferromagnet in three dimensions (3DIH) Eq. (2.11) immediately gives Eq. (A9), i.e., $\Delta(\omega)\propto\omega^{1/2}$ for $\omega\to0$. It is clear in this case, and for any model spectrum of the form $\Delta\propto\omega^s$ in this limit, with $0<s<1$, that the integral (5.4) is divergent and the initial susceptibility $\chi$ is infinite.

To make further investigations more quantitative, we should concentrate on the function $\sigma(T,H)$ for small $H$. Let us take the virtual spectrum in a rather general form,

$$\Delta(\omega)=\begin{cases}\Theta(\omega)\omega^s\Delta_a(\omega)\equiv\Theta(\omega)\omega^s\sum\limits_{m=0}^{\infty}D_m\omega^m, & \text{for } \omega<\omega_n\\ \text{aribitrary, integrable function of } \omega, & \text{for } \omega_n<\omega<\omega_m\\ 0, \quad \text{for } \omega_m<\omega\ , & \end{cases} \tag{5.5}$$

where $\omega_n$ is the lowest nonzero point of nonanalyticity of $\Delta(\omega)$, $\omega_m=\max\omega_q$, and for the power index $s$ there is $0<s<1$. Note that such a form of $\Delta(\omega)$ with $s=\frac{1}{2}$ corresponds to the 3DIH ferromagnet; see Appendix A.

The freedom of having $s$ different from this value turns out to be useful for a description of magnetic phenomena near $T_C$. Note that the spectrum with a gap, $\Delta(\omega)=0$ for $0<\omega<\omega_n$, is also covered by this general form—one obtains it by setting $D_m=0$, $m=0,1,2,\ldots$ .

Evaluation of the integral (3.4) with the preceding spectrum, at small $H$, has been done in Appendix C. On solving iteratively Eq. (C4) we obtain the following form of the $\sigma$ versus $H$ dependence, valid for $0<T<T_C$:

$$\frac{\sigma(T,H)-\sigma(T,0)}{\sigma(T,0)}=\frac{2\pi D_0 T}{\sin(\pi s)\Phi(\sigma_0,T)\sigma_0\kappa(\sigma_0)}\times\left[\frac{\mu H}{\sigma_0\kappa(\sigma_0)}\right]^s+O(H^{2s},H^1)\ , \quad (5.6)$$

where $\sigma_0$ and $\Phi$ are defined by Eqs. (5.2) and (5.3) and $D_0$ is the coefficient of the leading term of the analytic factor in the expansion (5.5). We can see that for $H\to 0$ the field-induced increase of the magnetization has a nonanalytic form $\propto H^s$, with the power index $s$ as in the nonanalytic factor of the virtual spectrum (5.5). For the 3DIH ferromagnet the magnetization increase goes as $H^{1/2}$, i.e., as found by Holstein and Primakoff[1] for the limit $T\to 0$. However, our result is valid at all temperatures below $T_C$, both in the RPA, $\kappa=1$, and in the MCRPA approach.

## VI. LOW-$T$ EXPANSION OF MAGNETIZATION

It is interesting to compare the higher-order terms of the magnetization expansion with respect to $T$, for low $T$, with the exact terms derived elsewhere. An expansion procedure for Eq. (3.4), appropriate for this purpose, has been presented in Appendix D. Function $P$ given in the form (D1) of this equation has been calculated—see Eq. (D16)—assuming the virtual spectrum (5.5). Factor $\sigma\kappa(\sigma)$, appearing in the first argument of this function, can be expanded with respect to the quantity $\sigma-1$, which is small for $T\to 0$,

$$\kappa_1\equiv\kappa(1),\quad \kappa_1'\equiv d\kappa/d\sigma \quad \text{at } \sigma=1\ ,$$

$$\sigma\kappa(\sigma)=\kappa_1[1+(1+\kappa_1'/\kappa_1)(\sigma-1)+O((\sigma-1)^2)]\ . \quad (6.1)$$

On solving Eq. (D1) with the help of (D16) and (6.1) we obtain

$$\begin{aligned}\sigma(T,H)=1&-2[D_0\Gamma(1+s)Z_{1+s}(x)y^{1+s}+D_1\Gamma(2+s)Z_{2+s}(x)y^{2+s}+D_2\Gamma(3+s)Z_{3+s}(x)y^{3+s}+O(T^{4+s})]\\&+4\{[1-(1+s)(1+\kappa_1'/\kappa_1)][D_0\Gamma(1+s)]^2[Z_{1+s}(x)]^2y^{2+2s}\\&+[2-(3+2s)(1+\kappa_1'/\kappa_1)]D_0\Gamma(1+s)D_1\Gamma(2+s)Z_{1+s}(x)Z_{2+s}(x)y^{3+2s}+O(T^{3+3s})\}\ ,\\&x=\mu H/T\quad y=T/\kappa_1\ . \quad (6.2)\end{aligned}$$

We can see that the low-temperature expansion of the magnetization is determined in full by the constants $D_0,D_1,D_2,\ldots$, and by the power index $s$ of the low-frequency part of the spectrum (5.5), and by the decoupling factor $\kappa(\sigma)$ and its first derivative, both taken at $\sigma=1$. With $\kappa_1=1$ and $\kappa_1'=0$ this MCRPA formula turns into the RPA formula, such as given by Tyablikov,[4] although it should be noted that our coefficients $D_m$ have been defined in a general way—Eqs. (A10)-(A14)—whereas those in Ref. 4 concern cubic lattices with nearest-neighbor interactions only.

Amazingly, in the mentioned work there is not an explicit form of the $\sigma$ versus $H$ dependence in the $H\to 0$ limit; the function $Z_\alpha(\mu H/T)$ [defined in Eq. (D13)], appearing in Ref. 4 and in Eq. (6.2), is in fact somewhat difficult to analyze in this limit. We have been able to complete this point using Eq. (D15); the leading terms of the expansion at small $T$ and $H/T$ are

$$\sigma(T,H)=1-2D_0\Gamma(\tfrac{3}{2})\left[\zeta(\tfrac{3}{2})-2\pi^{1/2}\left[\frac{\mu H}{T}\right]^{1/2}+O\left[\frac{\mu H}{T}\right]\right]T^{3/2}+O(T^{5/2})\ . \quad (6.3)$$

We can see that the Holstein-Primakoff low-temperature result, following from the spin-wave mechanism of magnetic excitations, is hidden in the formula (3.4). It lends credibility to the RPA and MCRPA predictions in the whole ferromagnetic region of temperatures.

Being still within the 3DIH model, we can compare Eq. (6.2) with the exact low-temperature expansion derived by Dyson.[10] His result consists of two parts: a contribution due to independent spin waves, given here in Eq. (D18), and a correction due to dynamical spin-wave interaction, which in the present notation can be nicely written as

$$\sigma_{\rm dyn}=-8Q\left[D_0\Gamma(\tfrac{3}{2})Z_{3/2}\left[\frac{\mu H}{T}\right]T^{3/2}\right]\times\left[D_1\Gamma(\tfrac{5}{2})Z_{5/2}\left[\frac{\mu H}{T}\right]T^{5/2}\right]+O(T^5)\ . \quad (6.4)$$

The value of $Q$, according to Dyson, is between 1.35 and 1.68 (for cubic lattices and $S=\frac{1}{2}$). The so-called kinematical interaction leads to corrections that are exponentially small and negligible.

We see, that in order to have the terms in the first set of square brackets in (6.2) equal to the initial terms of the Dyson formula (D18) for spin $S=\frac{1}{2}$, we should set the power index $s=\frac{1}{2}$ and choose the value of the decoupling factor at $\sigma=1$ to be

$$\kappa_1\equiv\kappa(1)=1\ . \quad (6.5)$$

The terms in the curly brackets of (6.2) correspond to the dynamical interaction contribution (6.4). We see that

(6.2) contains a spurious term $\propto T^3$, absent in (6.4). It turns out that one can eliminate this term by choosing the derivative of the coupling factor at $\sigma=1$ to be

$$\kappa_1' = -s\kappa_1/(s+1) \ . \tag{6.6}$$

Our term $\propto T^4$ has exactly the same field dependence $\propto Z_{3/2}(\mu H/T) Z_{5/2}(\mu H/T)$ as the Dyson term (6.4). On inserting (6.5) and (6.6) into its coefficient we obtain, in our case,

$$Q_{\rm MCRPA} = \tfrac{1}{3} \ , \tag{6.7}$$

i.e., the coefficient has the same sign as the Dyson's, although it is 4–5 times smaller.

We have therefore found that within the MCRPA (but not RPA) it is possible to eliminate the $T^3$ term, while retaining the $T^4$ term, although its coefficient is too small. However, in this work we shall not exploit this point any further.

## VII. EQUATION OF STATE NEAR $T_C$

In this section we shall find the form of the equation of state in the MCRPA in close proximity to the $T_C$. In this region the static-scaling theory is valid, and one may ask whether the present theory can match it and in which way. Indeed, this can to a great extent be achieved with a proper choice of the decoupling factor $\kappa(\sigma)$ and of the model virtual spectrum $\Delta(\omega)$.

When $T$ approaches $T_C$, the formula (5.6) becomes meaningless, because its denominator tends to zero; we need a more subtle treatment; see Appendix E. In this region the temperature dependence of the decoupling factor $\kappa$ becomes important. It is our ansatz that it enters only through the relative magnetization $\sigma$. In accordance with the discussion in Sec. II and with Eqs. (3.5) and (6.5), and having in mind some further steps, we postulate $\kappa(\sigma)$ in the following form:

$$\begin{gathered}\kappa(\sigma) = \kappa_0(1 + b\sigma^2 - c|\sigma|^p) \ , \\ 1 + b - c = 1/\kappa_0, \quad 2 < p < 4 \ .\end{gathered} \tag{7.1}$$

These are the values of the coefficients $b$ and $c$, together with the power index $p$, that determine within the MCRPA the values of some critical indices, as will be shown later. Such an ansatz is in the spirit of the Onsager reaction-field correction of the mean-field theory of magnetism,[12] as one can see best by applying the form (7.1) in Eq. (3.4a).

The general form of the MCRPA equation of state (3.4) has in Appendix E been transformed into a combination (E6) of power series in variables, which are small in the critical region. This equation, with the $\kappa(\sigma)$ of Eq. (7.1) inserted, will now be rewritten in terms of the variables $\sigma$, $H/\sigma$, and $t$ [see (E5)], and the accuracy will be limited only to the leading terms of the expansions involved. One obtains

$$\begin{aligned}&\langle \omega^{-1} \rangle [t + (\tfrac{1}{3}\langle \omega^{-1} \rangle \langle \omega \rangle - b)\sigma^2 + c|\sigma|^p] \\ &\quad = \frac{D_0 \pi}{\sin(\pi s)} \left[ \frac{\mu H}{\sigma \kappa_0} \right]^s + g_1^{\rm BR} \left[ \frac{\mu H}{\sigma \kappa_0} \right]^1, \quad t = \frac{T - T_C}{T_C} \ .\end{aligned} \tag{7.2}$$

A general idea behind this form is that of the two terms on the LHS, $\propto \sigma^2$ and $\propto |\sigma|^p$, only one is to be left; the same takes place for the terms $\propto H^s$ and $\propto H^1$. The actual choice depends on the coefficients of these terms, which can be zero or not. This point is crucial for this paper—it is the freedom in choosing the parameters $b,c$ of $\kappa(\sigma)$, which makes it possible to adjust the MCRPA critical index $\beta$ to the value following from experiment or derived with the renormalization-group (RG) methods.

We can cover all possible cases with a single formula by writing

$$\langle \omega^{-1} \rangle (t + Q_p |\sigma|^p) = R_s \left[ \frac{\mu H}{\sigma \kappa_0} \right]^s , \tag{7.3}$$

where the notation for the RHS is (i) if the virtual spectrum shows a gap at low frequencies, i.e., $D_m = 0$ for $m = 0, 1, \ldots$, then [see (C35)]

$$s = 1, \quad R_s = \langle \omega^{-2} \rangle \ , \tag{7.4a}$$

or (ii) if $D_0 > 0$ in the spectrum (5.5), then

$$0 < s < 1, \quad R_s = \pi D_0 / \sin(\pi s) \ . \tag{7.4b}$$

The notation for the LHS is (i) if $c = 0$, $b = 1/\kappa_0 - 1$,

$$b < [\langle \omega^{-1} \rangle \langle \omega \rangle / 3] \ ,$$

then

$$p = 2, \quad Q_p = \langle \omega^{-1} \rangle \langle \omega \rangle / 3 - b \ , \tag{7.5a}$$

or (ii) if $b = \langle \omega^{-1} \rangle \langle \omega \rangle / 3$, $c = 1 + b - 1/\kappa_0$, $c > 0$, then

$$2 < p < 4, \quad Q_p = c \ . \tag{7.5b}$$

It is clear from the above, that depending on our choice of the coefficients $b,c$ and $D_0$,$s$ we can have essentially different models of ferromagnetism.

## VIII. SCALING EQUATION

The last form of the equation of state (7.3) can be transformed into the form typical for the static-scaling theory (see Ref. 2, and references therein). Depending on the choice of the coefficients $b$ and $c$ [related to the formal index $p$, see (7.5)], and on the properties of the $\Delta(\omega)$ [related to the formal index $s$, see (7.4)] we can have many kinds of critical behavior, each represented by an equation of the form of a scaling equation

$$\begin{gathered} y = x \left[ \frac{\langle \omega^{-1} \rangle}{R_s} \right]^{1/s} (Q_p x^p + \mathrm{sgn}(t))^{1/s} \ , \\ (p=2) \vee (2 < p < 4), \ (s=1) \vee (0 < s < 1) \ , \end{gathered} \tag{8.1}$$

where

$$x = \sigma / |t|^{1/p}, \quad y = \mu H / |t|^{(p+s)/p/s} \ , \tag{8.2}$$

and $\sigma \geq 0$ and $H \geq 0$ have been assumed. Consequently, on comparing $x$ and $y$ defined by (8.2) with the same variables defined within the static-scaling theory using the critical indices, we have established the following relations between the critical indices and the MCRPA parameters $s$ and $p$:

$$\beta=1/p, \quad \Delta=(p+s)/p/s, \quad \delta=1+p/s, \quad \gamma=1/s \ . \qquad (8.3)$$

Customarily, one writes the scaling equation in the form $x=W(y)$, where $W$ is the so-called scaling function.[2] Equation (8.1), being of the form $y=W^{-1}(x)$, therefore gives the (inverse) scaling function. It has been derived here, for the first time it seems, from first principles.

Six sets of the parameters and critical indices, characterizing six types of the MCRPA models of ferromagnetism, have been shown in Table I.

We can see that the MCRPA offers many possible models, and one needs an independent guide to choose some. This can be either an experiment or suggestions from an independent theory, such as the renormalization-group theory[2] (RG). As an example, we have take the values $\beta=0.3647$ and $\gamma=1.3866$, determined for the isotropic Heisenberg system by Le Guillou and Zinn-Justin[13] using the RG methods, and used them to calculate, via Eqs. (8.3), the parameters $s$ and $p$ of the present theory: $s=0.721\,18$ and $p=2.742$. The same has been done for the Ising system, assigned here to $s=1$; with $\beta=0.325$ one gets the value $p=3.077$. For the Ising system there is no similar way to manipulate the critical index $\gamma$ in order to adjust it to experimental or RG values; it is just $\gamma=1$ here, as in the mean-field approximation (MFA).

We may consider the so-obtained numbers as giving us some information on the $\langle S_l^z S_{l'}^z \rangle$ correlation function, via Eqs. (7.1) and (2.8), and on the virtual spectrum [i.e., the density of states, see (3.3)] at low energies, via (5.5). The number $s=0.721\,18$ differs considerably from the value $s=\frac{1}{2}$, following from the formula (A9) for the 3DIH magnet. This may be an artifact, due to our forced implantation of the RG result onto the RPA scheme. On the other hand, we may consider it as an indication of the temperature-induced renormalization of the energy spectrum of ferromagnets near the transition temperature, as compared with the spectrum near $T=0$. In any case, the idea of an interrelation between the microscopic parameters $s,p$ and the indices of the scaling theory is important and enlightening.

The six models described earlier, characterized by various sets of mutually interrelated parameters and indices, have been presented in Table I. Some experimental figures are also shown. Interestingly, the indices in the original RPA model for the 3DIH system (type 3, with $s=\frac{1}{2}$ and $\kappa=1$) are the same as for the spherical model.[14]

## IX. SPONTANEOUS MAGNETIZATION FOR SOME MCRPA MODELS

In this section we report the results of numerical calculations of the magnetization for several MCRPA models exhibiting the renormalization-group-imposed critical indices, and compare these $\sigma$ versus $T$ plots with the corresponding Weiss and RPA plots, treated here as reference plots.

It is convenient to express characteristic frequencies of virtual spectra and temperature in units of the critical temperature $T_C$. Various virtual spectra with a gap at $\omega=0$ (types 1 and 2 in Table I) are expected to result in similar magnetic behavior. (Some such spectra are discussed in Sec. III and Appendix B in connection with the

TABLE I. MCRPA indices $s$ and $p$, and critical indices for six types of models.

| nr | Type of model | $s$ | $p$ | $\beta$ | $\delta$ | $\gamma$ | $\gamma'$ |
|---|---|---|---|---|---|---|---|
| | Spectrum with gap at $\omega=0$ | | | | | | |
| 1 | Weiss-Ising RPA imposed $\kappa$ | 1 | 2 | 0.5 | 3 | 1 | 1 |
| 2 | RG imposed $\beta$ | 1 | 3.077 | 0.325[a] | 7.154 | 1 | 1 |
| | Gapless spectrum | | | | | | |
| 3 | RPA imposed $\kappa$ 3DIH imposed $s$ | 0.5 | 2 | 0.5 | 5 | 2 | |
| 4 | RG imposed $\beta$ 3DIH imposed $s$ | 0.5 | 2.742 | 0.3647[a] | 6.484 | 2 | |
| 5 | RG imposed $\gamma$ RPA imposed $c$ | 0.7212 | 2 | 0.5 | 3.771 | 1.3866[a] | |
| 6 | RG imposed $\beta$ and $\gamma$ | 0.7212 | 2.742 | 0.3647[a] | 4.802 | 1.3866[a] | |
| | Experimental (Ref. 21) | | | | | | |
| | Ni | | | 0.378 | 4.58 | 1.34 | |
| | Fe | | | 0.389 | 4.35 | 1.33 | |
| | | | | 0.37 | | 1.30 | |
| | Co | | | 0.36 | | 1.23 | |
| | Ga | | | 0.38 | 3.61 | 1.19 | |

[a]From Ref. 13.

TABLE II. Parameters of the decoupling factor $\kappa$, (7.1) and of the model virtual spectra for various models of the MCRPA theory of ferromagnetism. These models correspond to the six model types of Table I. $\rho_0=2(1+\gamma)(4+8\gamma+\gamma^2)/(1+2\gamma)/3$.

| nr | Model | $\kappa_0$ | $b$ | $c$ | $\rho$ |
|---|---|---|---|---|---|
| | Ising spectrum (4.1) $\omega_I=\rho T_C$, $s=1$, $\langle\omega^n\rangle=\omega_I^n$ | | | | |
| 1 | Weiss-Ising (WI) RPA-imposed $\kappa$, $p=2$ | 1 | 0 | 0 | 2 |
| 2 | RG-imposed $\beta=0.325$, $p=1/\beta$ | $2/\rho$ | $\frac{1}{3}$ | $(8-3\rho)/6$ | $<\frac{8}{3}$ |
| | Debye spectrum (9.1) $\omega_m=\rho T_C$, $0<s<1$ $\langle\omega^{-1}\rangle=(s+1)/s/\omega_m$ $\langle\omega\rangle\langle\omega^{-1}\rangle=(s+1)^2/s/(s+2)$ | | | | |
| 3 | RPA-imposed $\kappa$ 3DIH-imposed $s=\frac{1}{2}$ | 1 | 0 | 0 | 6 |
| 4 | RG-imposed $\beta=0.3650$, $p=1/\beta$ 3DIH-imposed $s=\frac{1}{2}$ | $6/\rho$ | $\frac{3}{5}$ | $(48-5\rho)/30$ | $<\frac{48}{5}$ |
| 5 | RG-imposed $\gamma=1.3866$, $s=1/\gamma$ RPA-imposed $c$, $p=2$ | $2(1+\gamma)/\rho$ | $\rho/(1+\gamma)/2-1$ | 0 | $<\rho_0$ |
| 6 | RG-imposed $\beta$ and $\gamma$, $p=1/\beta$, $s=1/\gamma$ | As above | $(1+\gamma)^2/(1+2\gamma)/3$ | $1+b-1/\kappa_0$ | $<\rho_0$ |

paramagnetic susceptibility.) To represent them we take the Ising virtual spectrum (4.1), and characterize such models by the dimensionless parameter $\rho=\omega_I/T_C$.

For models based on gapless spectra (types 3–6 of Table I) we take the Debye-like spectrum of a power-law type

$$\Delta(\omega)=D_0\omega^s\Theta(\omega)\Theta(\omega_m-\omega)\ , \tag{9.1}$$

where $D_0=(s+1)/\omega_m^{s+1}$, characterized by two parameters—the power index $s$ and the cutoff energy $\omega_m$; $\rho=\omega_m/T_C$. Other simple spectra of this type (not considered here) might be the gapless elliptic one and the gapless singular one, both shown in Table III. We should emphasize that the main reason for choosing (9.1) as our model spectrum is that it is the simplest spectrum of the (5.5) type, i.e., the one having the power-law behavior at low frequencies. It may differ significantly from real spectra not only in different shape at higher frequencies, but also at low frequencies—the value of $D_0$ in (9.1), which is imposed by the normalization condition, may be quite different from $D_0$ following from the dispersion relations $\omega_{\mathbf{q}}$ at small wave vectors $\mathbf{q}$ [see Eqs. (A9), (A10), and (A2)].

Having established the virtual spectrum, we can determine other relevant parameters for the six model types of Table I; they are given in Table II. The corresponding $\sigma(T,0)$ plots are shown in Figs. 3 and 4. Figure 3 shows the MFA spontaneous magnetization curves adjusted, via $\kappa(\sigma)$, to exhibit the RG critical exponent[13] for the Ising system, $\beta=0.325$ (model 2). Clearly, they are steeper near $T_C$ than the classic Weiss curve (labeled WI, model 1), with $\beta=\frac{1}{2}$. The overall magnetization turns out to be quite sensitive to the choice of the parameter $\rho=\omega_I/T_C$. The plots of the decoupling factor $\kappa[\sigma(T,0)]$, shown in the inset, display its strong variation with temperature (except for $\rho=2$, the same as the WI case). There is a tendency of $\kappa$ to increase for $T\to T_C$. This may be interpreted as a tendency of three-spin correlation functions for the Ising systems to decrease in this limit slower—see

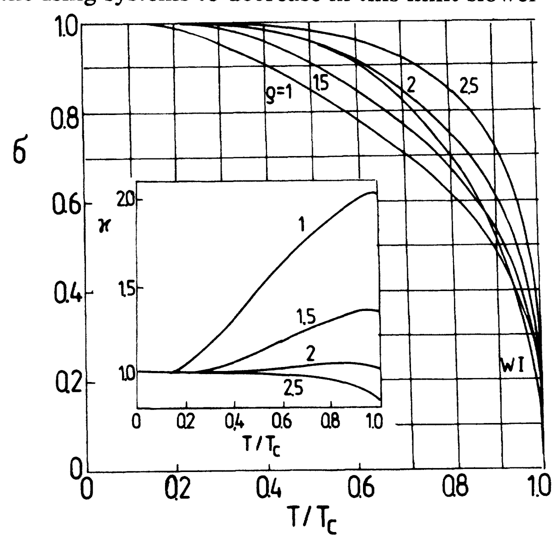


FIG. 3. Spontaneous magnetization $\sigma(T,0)$ vs $T/T_C$, assuming virtual spectrum $\Delta(\omega)=\delta(\omega-\omega_I)$, i.e., the MFA. Curve WI—classic Weiss Ising plot, solution of Eq. (4.3) at $H=0$ with $\kappa=1$, (model 1 of Tables I and II); here $\beta=\frac{1}{2}$. The remaining curves represent model 2 of these tables. It is the MFA model with the decoupling factor $\kappa$, Eq. (7.1), chosen so that the critical index $\beta=0.325$, the renormalization-group value for Ising case. The curves are labeled by the corresponding values of the parameter $\rho=\omega_I/T_C$. Appropriate $\kappa[\sigma(T,0)]$ plots are shown in the inset.

Eq. (2.6)—than the corresponding product of the magnetization and relevant two-spin correlation functions would.

Now let us approach the magnetization of the systems with gapless virtual spectra. For the Debye-like spectrum (9.1) the comparison of the classic RPA magnetization curves with the predictions of the MCRPA, Eq. (3.4), adjusted to exhibit the RG critical indices near $T_C$, is presented in Fig. 4. Clearly, the RG corrections push $\sigma$ to much higher values than those occurring in the RPA, which is in accord with experimental trends. This increase is quite substantial even if one takes into account the critical index $\gamma$ only; see the curve RG$\gamma$. It should be emphasized that with such $\gamma$ we have a deviation of the low-temperature magnetization $1-\sigma \propto T^{1+s}$, $s=1/\gamma$, from the famous Bloch $T^{3/2}$ law. Indeed, the power index $1+s=1.7212$, see the tables, which should be compared with 1.5 for $s=\frac{1}{2}$, the spin-wave-model value for the 3DIH system. The difference, although small from the point of view of ordinary experimental accuracy (see, e.g., Fig. 5 for Ni), may have a profound meaning. In the RG$\gamma$ case the $\beta$ index still has its MFA value $\frac{1}{2}$, while the RG$\beta\gamma$ curve exhibits the critical behavior, $\sigma \propto (T_C-T)^{\beta}$, characterized by the RG $\beta=0.3647$. The value $\rho=6$, dictated by the $\kappa=1$ of the RPA, is optional in the MCRPA; in the next section this freedom will be exploited to achieve a good fit of the model curves to the experimental data for Ni.

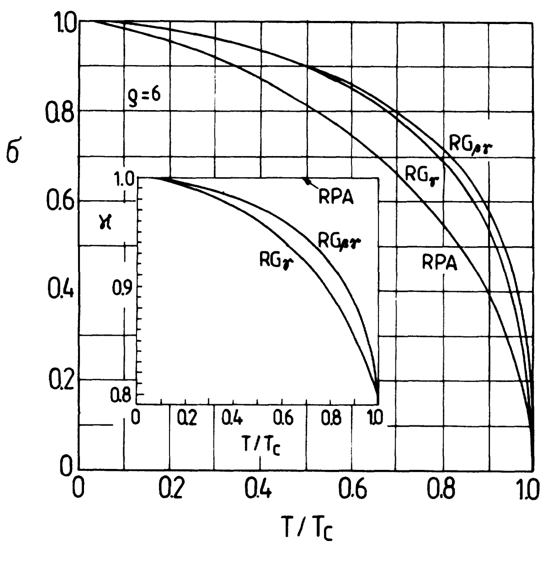


FIG. 4. Spontaneous magnetization $\sigma(T,0)$ vs reduced temperature $T/T_C$, assuming the Debye-like power-law form of the virtual spectrum, Eq. (9.1). The curve labeled RPA follows from the original BT equation (3.4) with $\kappa=1$ and the spectrum index $s=\frac{1}{2}$ (the value such as for 3DIH Hamiltonian), model 3 of the tables. Remaining curves correspond to the MCRPA models presented in the tables. Curve RG$\gamma$ is for model 5, in which the power index $s$ in the virtual spectrum is adjusted to lead to the critical index $\gamma=1.3866$ of the renormalization group for 3DIH Hamiltonian. In model 6, curve RG$\beta\gamma$, the critical indices $\beta=0.3647$ and $\gamma=1.3866$ of the RG have been imposed to determine the corresponding microscopic parameters $p$ and $s$, via Eqs. (8.3). Inset shows the corresponding $\kappa[\sigma(T,0)]$ plots. In all cases $\rho=6$.

The $\kappa[\sigma(T,0)]$ curves drop from 1 at $T=0$ to $\simeq 0.79$ at $T_C$. This agrees with the intuition of an enhanced decline of higher-order correlation functions near the transition point, as compared with the low-order ones—see Eq. (2.8). Note that for Ising systems an opposite tendency has also appeared, as mentioned earlier.

We should note here that model 3 does not correspond in full to the BT theory. Although we have here $\kappa=1$ and the power index of the virtual spectrum is $s=\frac{1}{2}$, our model spectrum (9.1) differs significantly from the exact spectrum (3.2) with the 3DIH dispersion law (A1), appearing in the BT theory.

## X. COMPARISON WITH EXPERIMENT FOR Ni

A magnet characterized by the localized spin $S=\frac{1}{2}$ does not possibly exist in nature, but at least nickel was once believed to be the case. This is, partly, why we have taken Ni for comparing its magnetic characteristics with predictions of the MCRPA models. It is also hoped that the exact value of $S$ is of secondary importance when one does not deal with the absolute value of the magnetization $M(T,H)$ but with the relative magnetization $\sigma=M(T,H)/M(0,0)$. Finally, as we have worked with the model forms of the virtual spectra (4.1) and (9.1), only the main features of the characteristics can be expected to be in agreement with experimental data. Only being aware of these inherent limitations, it is sensible to make the comparison. As we shall see, however, the result is better than anticipated.

In Fig. 5 we compare the MCRPA plots of the RG$\beta\gamma$ type for the spontaneous magnetization versus temperature with the experimental data for Ni, as collected in the

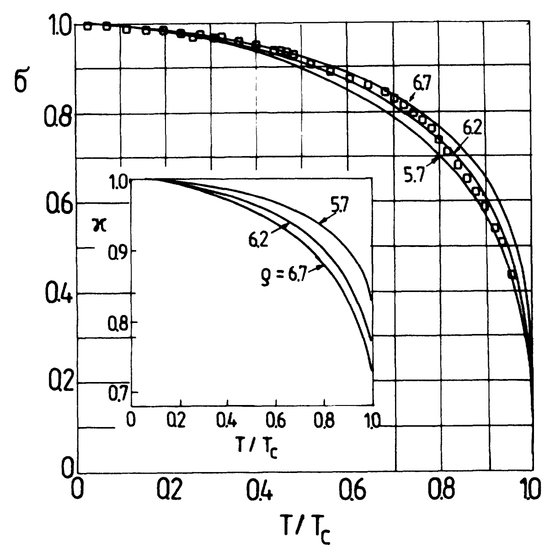


FIG. 5. Spontaneous magnetization of model 6 of the MCRPA, but with the RG critical indices replaced by the experimental values $\beta=0.378$, $\gamma=1.34$ for nickel, compared with the experimental points for the magnetization taken from Ref. 15. The only free parameter $\rho$ has been found to be 6.2 for the best fit. With the original RG parameters the deviations are $\sim 10\%$ larger and for best fit we have found $\rho=6.5$.

Landolt-Börnstein tables,[15] with $T_C=627.25$, according to Carre and Souletie.[16] An overall fit is rather good for the case $\rho=6.2$, although one must remember that at both limits $T\rightarrow 0$ and $T\rightarrow T_C$ taken separately the spin-wave theory and the RG approach, respectively, provide a better agreement. The virtue of the present result is, however, clear: It is perhaps the only plot, so far, in which the predictions of these two theories, so important from a conceptual point of view, have been (to a good approximation) united within the single interpolation scheme of microscopic origin. With a somewhat different $\rho$ one obtains a similar quality of the fit for Fe and Co.

True, there is a small discrepancy, mentioned in Sec. IX—at low temperatures the power index in $1-\sigma \propto T^{1+s}$, when calculated using the RG indices $\beta$ and $\gamma$ (or using experimental indices), differs a little from the spin-wave value $\frac{3}{2}$. This, however, is hardly visible within the pictorial accuracy of Fig. 5. Besides, we could easily remove this discrepancy, on introducing a phenomenologic interpolation such as

$$s=\tfrac{1}{2}+(1/\gamma-\tfrac{1}{2})\exp[-w(T-T_C)^2/(T_C T)]$$

(giving correct value at $T\rightarrow 0$, $T\rightarrow T_C$, and $T\rightarrow\infty$) into the MCRPA, if we were for the interpolation merits only.

The discrepancy between the experimental points and the MCRPA curves of the RG$\beta\gamma$ type in Fig. 5, seemingly small, turn out to be quite visible in the isotherms, $\sigma$ versus the scaled external field $h=\mu H/T_C$, near the critical temperature, as we show in Fig. 6. Here the experimental points have been taken from the paper by Weiss and Forrer[17] (corrected for demagnetization effects, according to them). We have used the experimental critical indices $\beta,\gamma$ of Kouvel and Comly[18] (with the original RG indices the deviations are slightly larger, $\sim 5\%$). The largest discrepancy appears in the critical isotherm, at $T_C$ (experimental data marked with $T/T_C=1.0005$ in Fig. 6), in spite of the fact that the critical index $\delta$, as calculated here from the experimental $\beta,\gamma$ (see Table I) via Eqs. (8.3), differs negligibly from the purely experimental $\delta$ given there, and from the corresponding RG value.

Most probably, it is the simplified power-law form of the virtual spectrum (9.1) with a wrong value of $D_0$, which manifests itself in the wrong factor $f$ in the form such as $\sigma\simeq f h^{1/\delta}$ for the critical isotherm. This occurs in spite of the fact that such a spectrum gives the index $\delta$ correctly (to the accuracy of $s$ discussed earlier).

An overall quality of the fit is fairly good. The deviations between the calculated curves and the experimental points decrease fast for temperatures departing up or down from the critical temperature. Characteristically, the existing deviations near $T_C$ are at all measured magnetic fields roughly the same as at $H=0$, Fig. 5, so the general trend of the magnetization changes as a function of the field is given properly.

In Fig. 7, in order to demonstrate the way in which the critical indices tend to show up in the MCRPA isotherms, we present three of the curves $\sigma(T,H)$, which were already shown in Fig. 6, but now we plot them versus $h^s$ for $T<T_C$ and versus $h^{s/(s+p)}$ for $T=T_C$. With such a scale, at a sufficiently small field, the straight line is expected. We can see that such a behavior covers

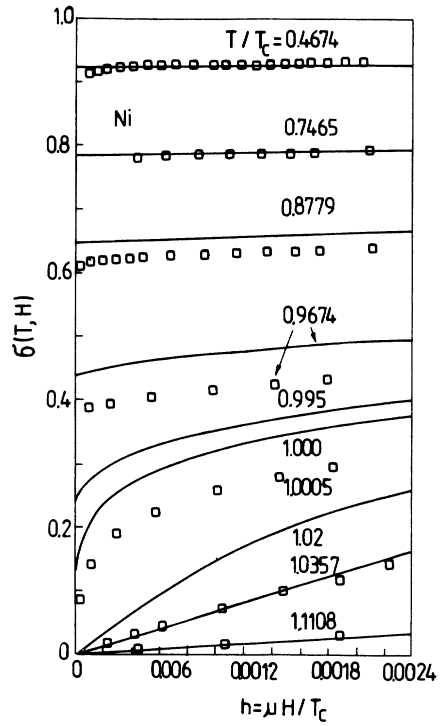


FIG. 6. Isotherms of magnetization $\sigma(T,H)$ vs external magnetic field (in the units of critical temperature), $h=\mu H/T_C$, model 6 of the MCRPA as characterized for Fig. 5, compared with the experimental data of Weiss and Forrer (Ref. 17). The curves and experimental points are labeled by corresponding reduced temperatures.

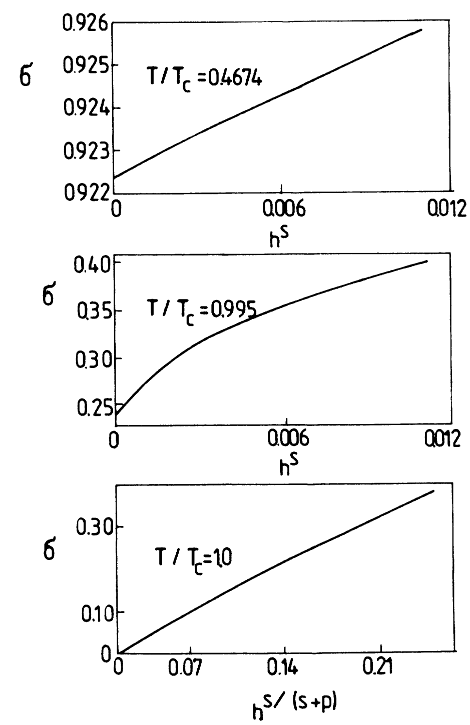


FIG. 7. Three isotherms $\sigma$ vs $h$ of Fig. 6, now plotted against $h^s$ for temperatures below $T_C$ (two upper curves) and against $h^{s/(s+p)}$ at the transition temperature, in order to demonstrate how wide the range of $H$ is, where the leading terms dominate in the expansions (5.6) and (7.3).

TABLE III. Inverse paramagnetic susceptibility $r(T)$ for some virtual spectra.

| Spectrum | $\Delta(\omega)$ | $r(T)$ | $T_C$ | $\gamma$ |
|---|---|---|---|---|
| Elliptic<br>width $2A>0$<br>gap $\xi A>0$ | $2\pi^{-1}A^{-2}x^{1/2}\Theta(x)$,<br>$x=A^2-(\omega-\xi A-A)^2$ | $2(T-T_C)(T-\psi^{-2}T_C)/T$,<br>$\psi=1+\xi+[(1+\xi)^2-1]^{1/2}>1$ | $A\kappa_0\psi/4$ | 1 |
| Gapless[a]<br>elliptic,<br>width $2A>0$ | $2\pi^{-1}A^{-2}x^{1/2}\Theta(x)$,<br>$x=\omega(2A-\omega)$ | $2(T-T_C)^2/T$ | $A\kappa_0/4$ | 2 |
| Singular,<br>width $A>0$<br>gap $\xi A>0$<br>$0<s<1$ | $A^{-1}\varphi_s\left[\frac{\omega-\xi A}{A}\right]$,<br>$\varphi_s(x)=\frac{\sin(s\pi)}{s\pi}$<br>$\times x^s(1-x)^{-s}\Theta[x(1-x)]$ | $2s^{-1}T_C\mu_s(\xi)$<br>$\times\left[\frac{[T-T_C\mu_s(\xi)]^{1/s}}{T^{1/s}-[T-T_C\mu_s(\xi)]^{1/s}}-\xi\right]$<br>$\mu_s(\xi)=1-\left[\frac{\xi}{1+\xi}\right]^s$ | $\frac{sA\kappa_0}{2\mu_s(\xi)}$ | 1 |
| Gapless[a]<br>singular,<br>width $A>0$ | $A^{-1}\varphi_s\left[\frac{\omega}{A}\right]$ | $2s^{-1}T_C\frac{(T-T_C)^{1/s}}{T^{1/s}-(T-T_C)^{1/s}}$ | $\frac{sA\kappa_0}{2}$ | $\frac{1}{s}$ |

[a]Such spectra were used in Ref. 22 in connection with some phonon problems.

almost the whole $h$ range at $T\simeq T_C/2$ and at $T_C$, but only a small part of this range for $T$ close to $T_C$. A small deviation from straight line is always present.

## XI. CONCLUSIONS

In the present theory—the MCRPA—the magnetization and related characteristics are given as a functional (3.4) of two functions—a virtual spectrum $\Delta(\omega)$, related to the spectrum of elementary excitations, and a decoupling factor $\kappa(\sigma)$, related to the three-spin correlation functions. Elementary mechanisms of interspin correlation and information on energy spectra of elementary magnetic excitations are in this versatile approach present to a degree sufficient to allow us to shape it, via some phenomenologic parameters, to fairly fit its predictions, for the magnetization versus $T$ and $H$ and the initial susceptibility versus $T$, with the experimental data or with the predictions of the renormalization-group theory.

Decoupling procedure for the three-spin Green's function in the equation of motion (2.5) for the two-spin GF $\langle\langle S(t),S(t')\rangle\rangle$ has been refined, as compared with the RPA theory,[3-5] on requesting the equality of first nonvanishing frequency moments. It has suggested to us that the decoupling factor $\kappa$ depends mainly on the relative magnetization $\sigma(T,H)$. The so-constructed moment-corrected RPA theory represents the long-needed interpolation scheme for the magnetization and the initial susceptibility of isotropic Heisenberg ferromagnets (and, to a lesser extent, for Ising ferromagnets), the scheme reasonable in the whole ($T$-$H$) plane.

In particular, one can choose the model decoupling factor (7.1) so that the magnetization near the Curie temperature exhibits the renormalization-group (or experimental) critical index $\beta$. Similarly, one can set up the virtual spectrum (5.5) so that the critical index $\gamma$ agrees with the RG or experimental values. There exist simple algebraic relations between the parameters $s,p$ of the MCRPA and the critical indices—Eqs. (8.3). The relation between the power index $s$ in the leading term of the assumed spectrum (5.5) and the critical index $\gamma$ for the susceptibility in paramagnetic region of temperature seems to be of a conceptual importance.

We have determined the behavior of magnetization versus the field $H$ at all temperatures. For $T<T_C$ it goes as

$$\delta\sigma=\sigma(T,H)-\sigma(T,0)\propto H^s ,$$

which turns into the Holstein and Primakoff[1] result $\delta\sigma\propto H^{1/2}$ in the case of the isotropic Heisenberg ferromagnet in three dimensions, at $T\rightarrow 0$. The equation of state in the critical region has the form (8.1) of the scaling equation. Thus we have derived, for the first time, it seems, the form of the scaling function $W(y)$ of the static scaling theory, both for the MCRPA and the RPA.

Using some model forms of the virtual spectrum in the MCRPA equation (3.4) we have been able to complete the integration involved and obtained analytic formulas for the magnetization and the susceptibility versus temperature, see, e.g., Eqs. (4.11) and (4.12), which are explicit and thus good for demonstration; see also Table III.

We show that the MCRPA-predicted magnetic characteristics at some special $T,H$ limits can be, on varying disposable parameters of the decoupling factor (7.1) and the spectrum (5.5), made identical with the exact values, calculated elsewhere from the Hamiltonian. Such possibility should not be pushed too far, however, because the too-short-blanket effect can appear—and improvement in one ($T$-$H$) region can result in a worsening of the fit in other regions. Without such a pressure, the MCRPA with a rather primitive model virtual spectrum gives for Ni a good description of the experimental situation in the $T$-$H$ plane—it becomes only fair near $T_C$, although the critical index is right.

Summing up, we have found that, starting from the anisotropic Heisenberg Hamiltonian, one can generalize the usual RPA theory of ferromagnetism, so that it provides a fair interpretation of magnetic phenomena at all fields and temperatures, including the critical phenomena. In this practical scheme all essential predictions are given in the form of relatively simple explicit formulas. We believe that with more sophisticated model functions $\Delta(\omega)$ and $\kappa(\sigma)$ an even better description of experiment is possible.

## APPENDIX A: VIRTUAL SPECTRUM OF THE THREE-DIMENSIONAL ISOTROPIC HEISENBERG MODEL AT LOW FREQUENCIES

The dispersion relation for virtual frequencies, Eq. (2.11), for the 3DIH ferromagnet, $J_l^{\|}=J_l^{\perp}=J_l$, takes on the form

$$\omega_{\mathbf{q}}=\tfrac{1}{2}\sum_{l\neq 0} J_l[1-\exp(i\mathbf{q}\cdot\mathbf{l})] \ . \tag{A1}$$

Here the range of interspin coupling is arbitrary. Assuming the inversion symmetry of the structure (as, e.g., in the case of all Bravais structures), and coupling isotropy: $J(-\mathbf{l})=J(\mathbf{l})=J(|\mathbf{l}|)$, we can rewrite it as follows:

$$\begin{aligned}\omega_{\mathbf{q}}&=-\tfrac{1}{2}\sum_{l} J_{|l|}\left[\frac{(i\mathbf{q}\cdot\mathbf{l})^2}{2!}+\frac{(i\mathbf{q}\cdot\mathbf{l})^4}{4!}+\frac{(i\mathbf{q}\cdot\mathbf{l})^6}{6!}+\cdots\right]\\&=C_2(\mathbf{n})q^2-C_4(\mathbf{n})q^4+C_6(\mathbf{n})q^6-\cdots \ ,\end{aligned} \tag{A2}$$

where

$$C_m(\mathbf{n})=\tfrac{1}{2}\frac{1}{m!}\sum_{l\neq 0} J_{|l|}(\mathbf{n}\cdot\mathbf{l})^m, \quad \mathbf{n}=\mathbf{q}/q \ . \tag{A3}$$

In order to determine the virtual spectrum $\Delta(\omega)$, in the definition (3.2) we replace the $\mathbf{q}$ summation by the integration over the Brillouin zone (BZ)

$$\begin{aligned}\Delta(\omega)&=\frac{v_{\text{at}}}{(2\pi)^3}\int_{\text{BZ}} d^3q\, \delta(\omega-\omega_{\mathbf{q}})\\&=\frac{v_{\text{at}}}{(2\pi)^3}\int_{4\pi} d^2\Omega_{\mathbf{n}}\int_0^{q_{\text{BZ}}(\mathbf{n})} dq\, q^2\delta(\omega-\omega_{\mathbf{q}}) \ .\end{aligned}$$

Here $v_{\text{at}}$ is the volume per one lattice site $\mathbf{l}$. Now we fix the direction $\mathbf{n}$ and change the variable $q$ (a scalar) into $x$ defined as

$$x=x(q)=C_2q^2-C_4q^4+C_6q^6-\cdots \ . \tag{A4}$$

This series can be inverted in a standard way,

$$q^2=A_1x^1+A_2x^2+A_3x^3+\cdots \ , \tag{A5}$$

where

$$A_1=C_2^{-1}, \quad A_2=C_4C_2^{-3}, \quad A_3=(2C_4^2-C_2C_6)C_2^{-5}, \ldots \ , \tag{A6}$$

and then differentiated:

$$\begin{aligned}q^2dq&=\tfrac{1}{2}(A_1x+A_2x^2+A_3x^3+\cdots)^{1/2}\\&\quad\times(A_1+2A_2x+3A_3x^2+\cdots)dx \ .\end{aligned} \tag{A7}$$

Having calculated the series for the square root and then for the product of two series, we finally get

$$\Delta(\omega)=\frac{v_{\text{at}}}{(2\pi)^3}\int d^2\Omega_{\mathbf{n}}\int_0^{x[q_{\text{BZ}}(\mathbf{n})]} dx\, \delta(\omega-x)\tfrac{1}{2}A_1^{3/2}x^{1/2}\left[1+\frac{5A_2}{2A_1}x+\left[\frac{7A_3}{2A_1}+\frac{7A_2^2}{8A_1^2}\right]x^2+\cdots\right] \ . \tag{A8}$$

Now for small $\omega$, i.e., less than min $x[q_{\text{BZ}}(\mathbf{n})]$, and within the convergence radius of the series in (A8), we can perform the integration with respect to $x$ and obtain

$$\Delta(\omega)=\omega^{1/2}(D_0+D_1\omega+D_2\omega^2+\cdots) \ , \tag{A9}$$

where the coefficients $D_m$ are given by the full solid angle integrals

$$D_0=\frac{v_{\text{at}}}{2(2\pi)^3}\int_{4\pi} d^2\Omega_{\mathbf{n}}[C_2(\mathbf{n})]^{-3/2} \ , \tag{A10}$$

$$D_1=\frac{v_{\text{at}}}{2(2\pi)^3}\int_{4\pi} d^2\Omega_{\mathbf{n}}\tfrac{5}{2}[C_2(\mathbf{n})]^{-7/2}C_4(\mathbf{n}) \ , \tag{A11}$$

$$D_2=\frac{v_{\text{at}}}{2(2\pi)^3}\int_{4\pi} d^2\Omega_{\mathbf{n}}\left\{\tfrac{63}{8}[C_2(\mathbf{n})]^{-11/2}[C_4(\mathbf{n})]^2-\tfrac{7}{2}[C_2(\mathbf{n})]^{-9/2}C_6(\mathbf{n})\right\} \ . \tag{A12}$$

For example, the cubic lattices we obtain

$$\begin{aligned}C_2(\mathbf{n})&=\tfrac{1}{4}\sum_{l} J_l(n_x^2l_x^2+n_y^2l_y^2+n_z^2l_z^2)=\tfrac{1}{4}\mathbf{n}^2\sum_{l} J_l\tfrac{1}{3}l^2\\&=\tfrac{1}{12}\sum_{l} J_l l^2\end{aligned} \tag{A13}$$

and, from (A10)

$$D_0=\frac{v_{\text{at}}}{(2\pi)^2}\left[\frac{12}{\sum_{l} J_l l^2}\right]^{3/2} \ . \tag{A14}$$

## APPENDIX B: PARAMAGNETIC SUSCEPTIBILITY VERSUS $T$ FOR SOME SPECIAL SPECTRA

Besides the rectangular spectrum (4.5), there are other virtual spectra $\Delta(\omega)$, for which Eq. (3.11) for the inverse paramagnetic susceptibility $r$ can be analytically integrated. In Table III we give the relevant formulas for a couple of them, the Curie temperatures calculated by requesting $r=0$, and the values of critical index $\gamma$.

## APPENDIX C: THE MCRPA EQUATION OF STATE AT FINITE $T$ AND SMALL $H$

To understand the field-dependence of the magnetization at finite temperatures of various magnetic systems, which may be described within the MCRPA, we have to make it explicit in the equation of state (3.4). This will be achieved now in the form of a power series in $H$. We do not assume $H$ to be infinitesimal—the only limitation is imposed by the radius of convergence of these series.

We assume the virtual spectrum (5.5). Three variables of our problem, $\sigma$, $H$, and $T$ appear in the RHS of Eq. (3.4) in two combinations only:

$$h=\frac{\mu H}{2T}\ , \tag{C1}$$

$$\lambda=\frac{\sigma\kappa(\sigma)}{2T}\ . \tag{C2}$$

While we are interested mainly in the small-$h$ expansions, we must allow the $\lambda$ to be arbitrary—it is large at low temperatures, although small around $T_C$ and above it. We rewrite Eq. (3.4) as

$$\sigma\langle\coth(h+\lambda\omega)\rangle-1=0\ , \tag{C3}$$

and then break up the term depending on $h$,

$$\sigma[F(\lambda)+G(\lambda,h)]-1=0\ , \tag{C4}$$

where

$$F(\lambda)=\langle\coth(\lambda\omega)\rangle\ , \tag{C5}$$

$$G(\lambda,h)=\langle\coth(h+\lambda\omega)-\coth(\lambda\omega)\rangle\ . \tag{C6}$$

It is convenient to introduce the $\coth(x)$ function with the $1/x$ singularity removed, i.e., the Langevin function

$$L(x)=\coth(x)-\frac{1}{x} \tag{C7}$$

having the obvious expansion

$$L(x)=\tfrac{1}{3}x-\tfrac{1}{45}x^3+\tfrac{2}{945}x^5-\cdots$$
$$=\sum_{m=0}^{\infty}c_{2m+1}x^{2m+1}\ , \tag{C8}$$

valid for $|x|<\pi$. Coefficients $c_n$ can be expressed in terms of the Bernoulli numbers. Using this function we can write (C6) as

$$G=G^{A}+G^{B}\ , \tag{C9}$$

with

$$G^{A}=\langle L(h+\lambda\omega)-L(\lambda\omega)\rangle\ , \tag{C10}$$

$$G^{B}=\left\langle\frac{1}{h+\lambda\omega}-\frac{1}{\lambda\omega}\right\rangle=\left\langle\frac{-h}{\lambda\omega(\lambda\omega+h)}\right\rangle\ . \tag{C11}$$

The $G^{A}(\lambda,h)$ is an analytic function of $h$ at $h=0$,

$$G^{A}(\lambda,h)=\sum_{n=1}^{\infty}\frac{1}{n!}G_n^{A}(\lambda)h^n\ , \tag{C12}$$

where

$$G_n^{A}(\lambda)=\left\langle\lim_{h\to 0}\left[\frac{\partial}{\partial h}\right]^n L(h+\lambda\omega)\right\rangle\ . \tag{C13}$$

For example,

$$G_1^{A}(\lambda)=\left\langle\frac{1}{(\lambda\omega)^2}-\frac{1}{\sinh^2(\lambda\omega)}\right\rangle\ . \tag{C14}$$

When investigating the $G^{B}$, we must separately examine the small frequency limit. We choose an arbitrary frequency $\Omega$ from the range $(0,\omega_n)$, where $\Delta(\omega)$ is given in the form (5.5), and split the integration range in (C11) into the lower (L) and upper (U) parts,

$$G^{B}=G^{BL}+G^{BU}\ , \tag{C15}$$

$$G^{BL}(\lambda,\Omega,h)=-\lambda^{-1}\int_0^{\Omega}d\omega\,\Delta(\omega)\omega^{-1}(1+\lambda h^{-1}\omega)^{-1}\ , \tag{C16}$$

$$G^{BU}(\lambda,\Omega,h)=\int_{\Omega}^{\infty}d\omega\,\Delta(\omega)[(h+\lambda\omega)^{-1}-(\lambda\omega)^{-1}]\ . \tag{C17}$$

The latter function is analytic in $h$,

$$G^{BU}(\lambda,\Omega,h)=\sum_{n=1}^{\infty}\frac{1}{n!}G_n^{BU}(\lambda,\Omega)h^n\ , \tag{C18}$$

$$G_n^{BU}(\lambda,\Omega)=\lim_{h\to 0}\left[\frac{\partial}{\partial h}\right]^n G^{BU}(\lambda,\Omega,h)$$
$$=n!(-1)^n\lambda^{-1-n}\int_{\Omega}^{\infty}d\omega\,\Delta(\omega)\omega^{-1-n}\ . \tag{C19}$$

On using the low-frequency expansion (5.5) for $\Delta(\omega)$ we rewrite (C16) as

$$G^{BL}=-\lambda^{-1}\sum_{m=0}^{\infty}D_m I(s+m,\Omega,h\lambda^{-1})\ , \tag{C20}$$

where we have introduced the function

$$I(\mu,\Omega,\xi)=\int_0^{\Omega}d\omega\,\omega^{\mu-1}(1+\xi^{-1}\omega)^{-1}\ , \tag{C21}$$

which can be expressed[19] in terms of the hypergeometric function $F(\alpha,\beta;\gamma;z)$ as

$$I(\mu,\Omega,\xi)=\mu^{-1}\Omega^{\mu}F(1,\mu;1+\mu;-\Omega\xi^{-1})$$
$$=\frac{\pi\xi^{\mu}}{\sin(\pi\mu)}+\frac{\Omega^{\mu-1}}{\mu-1}\xi F(1,1-\mu;2-\mu;-\xi\Omega^{-1})\ . \tag{C22}$$

Using this form, we can split the $G^{BL}$ into its nonanalytic (N) and regular (R) parts

$$G^{\mathrm{BL}}=G^{\mathrm{N}}+G^{\mathrm{BLR}}\ , \tag{C23}$$

$$G^{\mathrm{N}}(\lambda,h)=-\lambda^{-1}\sum_{m=0}^{\infty}D_m\frac{\pi}{\sin(\pi s+\pi m)}\left[\frac{h}{\lambda}\right]^{s+m}=-\lambda^{-1}\left[\frac{h}{\lambda}\right]^{s}\frac{\pi}{\sin(\pi s)}\sum_{m=0}^{\infty}D_m\left[-\frac{h}{\lambda}\right]^{m}\ , \tag{C24}$$

$$G^{\mathrm{BLR}}(\lambda,\Omega,h)=-\lambda^{-1}\sum_{m=0}^{\infty}D_m\frac{\Omega^{s+m-1}}{s+m-1}\left[\frac{h}{\lambda}\right]F\left[1,1-s-m;2-s-m;-\frac{h}{\lambda\Omega}\right]\ . \tag{C25}$$

Note that the nonanalytic part is already independent of the $\Omega$. On exploiting that

$$F(1,1-\mu;2-\mu;z)=\sum_{n=0}^{\infty}\frac{\mu-1}{\mu-1-n}z^n\ , \tag{C26}$$

we get, for the regular part the expression,

$$G^{\mathrm{BLR}}(\lambda,\Omega,h)=\frac{1}{\lambda}\sum_{n=1}^{\infty}\left[-\frac{h}{\lambda}\right]^n\sum_{m=0}^{\infty}\frac{D_m\Omega^{s+m-n}}{s+m-n}\ , \tag{C27}$$

which depends on $\Omega$, but when we combine it with the $G^{\mathrm{BU}}$, Eq. (C18), which is also regular and $\Omega$ dependent, we arrive at the sum, which is already $\Omega$ independent,

$$G^{\mathrm{BR}}(\lambda,h)=G^{\mathrm{BLR}}+G^{\mathrm{BU}}=\frac{1}{\lambda}\sum_{n=1}^{\infty}\frac{1}{n!}g_n^{\mathrm{BR}}\left[-\frac{h}{\lambda}\right]^n\ , \tag{C28}$$

because for the coefficient

$$\frac{1}{n!}g_n^{\mathrm{BR}}=\int_{\Omega}^{\infty}d\omega\,\Delta(\omega)\omega^{-1-n}+\sum_{m=0}^{\infty}\frac{D_m\Omega^{s+m-n}}{s+m-n} \tag{C29}$$

we immediately get

$$\frac{d}{d\Omega}\frac{1}{n!}g_n^{\mathrm{BR}}=-\Delta(\Omega)\Omega^{-1-n}+\left[\sum_{m=0}^{\infty}D_m\Omega^{s+m}\right]\Omega^{-1-n}=0\ .$$

Finally, we have obtained the equation of state (C4), with $F(\lambda)$ given by (C5), and $G(\lambda,h)$ in the form

$$G=G^{\mathrm{N}}+G^{\mathrm{BR}}+G^{\mathrm{A}} \tag{C30}$$

with

$$G^{\mathrm{N}}=-\frac{\pi}{\sin(\pi s)}\frac{1}{\lambda}\left[\frac{h}{\lambda}\right]^{s}\Delta_a\left[-\frac{h}{\lambda}\right]\ , \tag{C31}$$

where the $\Delta_a(\omega)$ is the analytic factor in the spectrum (5.5), and

$$G^{\mathrm{BR}}=\frac{1}{\lambda}\frac{1}{n!}\sum_{n=1}^{\infty}g_n^{\mathrm{BR}}\left[-\frac{h}{\lambda}\right]^n\ , \tag{C32}$$

$$G^{\mathrm{A}}=\sum_{n=1}^{\infty}\frac{1}{n!}G_n^{\mathrm{A}}(\lambda)h^n\ . \tag{C33}$$

As desired, in this form of the equation of state the $h$ dependence is explicit. The coefficients $g_n^{\mathrm{BR}}$, Eq. (C29), and $G_n^{\mathrm{A}}(\lambda)$, Eq. (C13), occurring in the regular part of $G$, depend on the $\Delta(\omega)$ in its full range of frequencies, while the nonanalytic part of $G$, Eq. (C31), involves the low-frequency part of $\Delta(\omega)$ only, namely, its analytic factor $\Delta_a(\omega)$ and the power index $s$, $0<s<1$, which defines the character of nonanalyticity of the spectrum.

It should be noted that the virtual *spectrum with a gap* at low frequencies, $\Delta(\omega)=0$ for $0\le\omega<\omega_n$, (e.g., such as for the Ising model) is represented by the formula (5.5) with $\Delta_a(\omega)=0$. It follows from Eq. (C31) that in such cases

$$G^{\mathrm{N}}=0\ . \tag{C34}$$

Therefore $G(\lambda,h)$ is an analytic function of $h$. The coefficients $g_n^{\mathrm{BR}}$ of the $G^{\mathrm{BR}}$ expansion (C29) turn in this case into the moments of the virtual spectrum

$$\frac{1}{n!}g_n^{\mathrm{BR}}=\langle\omega^{-1-n}\rangle\ . \tag{C35}$$

## APPENDIX D: EQUATION OF STATE FOR $T \ll T_C$

We shall examine here the MCRPA equation of state (3.4), looking for its explicit dependence on $T$ and $H$ in the region of very low temperature, and assuming the virtual spectrum of the general form given by Eq. (5.5). First we rewrite (3.4) as follows:

$$\sigma\left[1+2P\left[\frac{T}{\sigma\kappa(\sigma)},\frac{\mu H}{T}\right]\right]-1=0\ , \tag{D1}$$

where

$$P=\sum_{k=1}^{\infty}X_k\exp\left[-\frac{k\mu H}{T}\right]\ , \tag{D2}$$

$$X_k=\left\langle\exp\left[-\frac{k\sigma\kappa(\sigma)\omega}{T}\right]\right\rangle\ , \tag{D3}$$

using the obvious expansion

$$\coth(x)=1+2\sum_{k=1}^{\infty}\exp(-k2x),\quad x>0\ . \tag{D4}$$

In order to evaluate (D3) we split the integration range

$$X_k=X_k^{\mathrm{L}}+X_k^{\mathrm{U}}=\left[\int_0^{\Omega}+\int_{\Omega}^{\infty}\right]d\omega\,\Delta(\omega)\exp\left[-\frac{k\sigma\kappa\omega}{T}\right]\ , \tag{D5}$$

where $\Omega$ is an arbitrary fixed frequency from the range $(0,\omega_n)$. We note that the term $X_k^{\mathrm{U}}$ is exponentially small in $1/T$

$$X_k^{\rm U}=\exp\left[-\frac{k\sigma\kappa\Omega}{T}\right]\times\int_\Omega^\infty d\omega\,\Delta(\omega)\exp\left[-\frac{k\sigma\kappa(\omega-\Omega)}{T}\right] \tag{D6}$$

because the integral in (D6) is clearly less than one.

For $\Delta(\omega)$ given by (5.5) we can evaluate the term $X_k^{\rm L}$ analytically

$$X_k^{\rm L}=\sum_{m=0}^{\infty} D_m\int_0^\Omega d\omega\,\omega^{s+m}\exp\left[-\frac{k\sigma\kappa\omega}{T}\right]=\sum_{m=0}^{\infty} D_m\left[\frac{T}{\sigma\kappa k}\right]^{s+m+1}\left[\Gamma(s+m+1)-\Gamma\left[s+m+1,\frac{k\sigma\kappa\Omega}{T}\right]\right], \tag{D7}$$

where $\Gamma(\nu)$ and $\Gamma(\nu,u)$ are the complete and the incomplete gamma functions

$$\Gamma(\nu)=\Gamma(\nu,0)\ , \tag{D8}$$

$$\Gamma(\nu,u)=\int_u^\infty dx\,x^{\nu-1}e^{-x}\ , \tag{D9}$$

the latter having the following asymptotic expansion[19] for large $u$:

$$\Gamma(\nu,u)=u^{\nu-1}e^{-u}\left[\sum_{m=0}^{M-1}\frac{\Gamma(1-\nu+m)}{\Gamma(1-\nu)(-u)^m}+O\left[\frac{1}{u^M}\right]\right]. \tag{D10}$$

Therefore, in writing

$$X_k^{\rm L}=\sum_{m=0}^{\infty}\Gamma(s+m+1)D_m\left[\frac{T}{\sigma\kappa k}\right]^{s+m+1}+X_k^{\rm LE} \tag{D11}$$

the nonanalytic term exhibiting the $T$-power behavior has been separated from the $X_k^{\rm LE}$, which is exponentially small in $1/T$. On returning to (D2) we obtain

$$P=P\left[\frac{T}{\sigma\kappa(\sigma)},\frac{\mu H}{T}\right]=\sum_{m=0}^{\infty}\Gamma(s+m+1)D_m\left[\frac{T}{\sigma\kappa(\sigma)}\right]^{s+m+1}\times Z_{s+m+1}\left[\frac{\mu H}{T}\right]+\cdots\ , \tag{D12}$$

where

$$Z_\alpha(x)=\sum_{k=1}^{\infty}k^{-\alpha}e^{-kx}\ , \tag{D13}$$

and the ellipsis denotes here and throughout this appendix the terms that are exponentially small. Note that terms shown explicitly in (D12) are independent of the auxiliary parameter $\Omega$. The function (D13) can be written in terms of the special function $\Phi(z,s,v)$ defined in Ref. 20, p. 27,

$$Z_\alpha(x)=e^{-x}\Phi(e^{-x},\alpha,1)\ . \tag{D14}$$

Using its known expansion[20] we find

$$Z_\alpha(x)=\Gamma(1-\alpha)x^{\alpha-1}+\sum_{k=0}^{\infty}(k!)^{-1}\zeta(\alpha-k)(-x)^k\ , \tag{D15}$$

where $\zeta(x)$ is the Riemann's $\zeta$ function.

Therefore (D12) can be rewritten as follows:

$$P\left[\frac{T}{\sigma\kappa},\frac{\mu H}{T}\right]=\sum_{m=0}^{\infty}D_m\Gamma(s+m+1)\left[\frac{T}{\sigma\kappa}\right]^{s+m+1}\left[\Gamma(-s-m)\left[\frac{\mu H}{T}\right]^{s+m}+\sum_{k=0}^{\infty}\frac{\zeta(s+m+1-k)}{k!}\left[-\frac{\mu H}{T}\right]^k\right]+\cdots\ . \tag{D16}$$

Since $\Gamma(s+m+1)\Gamma(-s-m)=-(-1)^m\pi/\sin(s\pi)$, we can see that nonanalytic part of $2P$, Eq. (D16), is the same as $G^{\rm N}$, Eq. (C31), derived in a different way.

Equations (D1) and (D16) represent the equation of state, accurate to terms exponentially small in $1/T$. It has a form of the noninteger-power series in the variables $T/[\sigma\kappa(\sigma)]$ and $\mu H/T$.

Let us note that the preceding method applied, and the expression obtained for $P$, may be used also to evaluate the free energy $A$, and the magnetization $\sigma$, versus $T$ and $H$, of a perfect gas of independent (noninteracting) spin waves for the 3DIH ferromagnet, as introduced by Dyson[10]

$$A_{\rm indp}=E_0+T\left\langle\ln\left[1-e^{-(\mu H+2S\omega)/T}\right]\right\rangle=E_0-T\left[\sum_{m=0}^{\infty}Z_{m+\frac{5}{2}}\left[\frac{\mu H}{T}\right]D_m\Gamma(m+\tfrac{3}{2})\left[\frac{T}{2S}\right]^{m+\frac{3}{2}}+\cdots\right], \tag{D17}$$

$$\sigma_{\rm indp}=\frac{-1}{\mu S}\frac{\partial A_{\rm indp}}{\partial H}=1-\frac{1}{S}P\left[\frac{T}{2S},\frac{\mu H}{T}\right]=-\frac{1}{S}\left[\sum_{m=0}^{\infty}Z_{m+\frac{3}{2}}\left[\frac{\mu H}{T}\right]D_m\Gamma(m+\tfrac{3}{2})\left[\frac{T}{2S}\right]^{m+\frac{3}{2}}+\cdots\right], \tag{D18}$$

where

$$E_0=-\mu HS-\tfrac{1}{2}S^2\sum_l J_l\ , \tag{D19}$$

and $S$ is the spin value. Parameters $D_m$ have been calculated in Appendix A. The formulas (D17) and (D18) have exactly the same structure as those derived by Dyson.[10] However, the Dyson formulas were derived for cubic lattices with nearest-neighbor coupling, whereas here such restrictions are absent—the parameters $D_m$ are defined for arbitrary structure and interaction range.

We can see that in the light of the expansion (D15) the leading term in $H$ in the magnetization formula of Dyson is

$$\sigma(T,H)-\sigma(T,0)\propto H^{1/2}\ . \tag{D20}$$

It should be noted that for the virtual *spectrum with a gap* at low frequencies, $\Delta(\omega)=0$ for $0<\omega<\omega_n$, the function $X_k$ in Eqs. (D5) and (D6) is exponentially small, and therefore $\sigma(T,H)$ differs from 1 by such a small contribution.

## APPENDIX E: EQUATION OF STATE AT FINITE $T$ AND SMALL $\sigma$ AND $H$

We shall develop here a convenient form of the MCRPA equation of state for the critical region of temperatures, and for $T>T_C$. The equation of state (C4), supplemented by (C5), (C6), and (C30)–(C33), will be specified under the assumption of small $\sigma$. By this we mean that its dependence on $\sigma$ will be given in the form of power series; the magnitude of $\sigma$ is therefore limited only by the requirement of convergence.

Since $T$ is finite and so is $\kappa(\sigma)$, small $\sigma$ leads to small $\lambda$, Eq. (C2).

We therefore need to represent functions $F(\lambda)$ and $G_n^{\mathrm{A}}(\lambda)$ as power series. From Eqs. (C5)–(C8) we have

$$\begin{aligned}F(\lambda)&=\langle\coth(\lambda\omega)\rangle\\&=\left\langle\frac{1}{\lambda\omega}+\tfrac{1}{3}\lambda\omega-\tfrac{1}{45}(\lambda\omega)^2+\cdots\right\rangle\\&=\lambda^{-1}\langle\omega^{-1}\rangle+\sum_{m=0}^{\infty}c_{2m+1}\lambda^{2m+1}\langle\omega^{2m+1}\rangle\ ,\end{aligned} \tag{E1}$$

and from (C13) and (C8)

$$\begin{aligned}G_{2k}^{\mathrm{A}}(\lambda)&=\sum_{j=0}^{\infty}c_{2j+1+2k}\frac{(2j+1+2k)!}{(2j+1)!}\lambda^{2j+1}\langle\omega^{2j+1}\rangle\ ,\\G_{2k+1}^{\mathrm{A}}(\lambda)&=\sum_{j=0}^{\infty}c_{2j+1+2k}\frac{(2j+1+2k)!}{(2j)!}\lambda^{2j}\langle\omega^{2j}\rangle\ .\end{aligned} \tag{E2}$$

It is convenient to multiply the equation of state (C4) by $\kappa(\sigma)/(2T)$ to have the variable $\lambda$, Eq. (C2), there

$$\lambda F(\lambda)-\kappa(\sigma)(2T)^{-1}=-\lambda G(\lambda,h)\ . \tag{E3}$$

Now we make use of Eq. (3.6), and insert into (E3) the expansion (E1), to rewrite the following combination of its leading terms;

$$\begin{aligned}\langle\omega^{-1}\rangle-\frac{\kappa(\sigma)}{2T}&=\frac{\kappa_0}{2T_C}-\frac{\kappa(\sigma)}{2T}=\frac{T-T_C}{T_C}\frac{\kappa_0}{2T}-\frac{\kappa(\sigma)-\kappa_0}{2T}\\&=\left[t-\frac{\kappa(\sigma)-\kappa_0}{\kappa_0}\right]\frac{\kappa_0}{2T_C(1+t)}\ ,\end{aligned} \tag{E4}$$

where, following habits of the static-scaling theory,[2] we have introduced the scaled deviation from the critical temperature

$$t=(T-T_C)/T_C,\ \ T=T_C(1+t)\ . \tag{E5}$$

Finally, we arrive at the following form of the equation of state:

$$\left[t-\frac{\kappa(\sigma)-\kappa_0}{\kappa_0}\right]\frac{\kappa_0}{2T_C(1+t)}+\lambda^2[\tfrac{1}{3}\langle\omega\rangle-\tfrac{1}{45}\langle\omega^3\rangle\lambda^2+O(\lambda^4)]=-\lambda G\ , \tag{E6a}$$

where the RHS, according to Eqs. (C30)–(C33) and (E2), is

$$\begin{aligned}-\lambda G(\lambda,h)=&\frac{\pi}{\sin(\pi s)}\left[\frac{h}{\lambda}\right]^s\left\{D_0-D_1\left[\frac{h}{\lambda}\right]^1+O\left[\left[\frac{h}{\lambda}\right]^2\right]\right\}+\left[\frac{h}{\lambda}\right]^1\left\{g_1^{\mathrm{BR}}-g_2^{\mathrm{BR}}\left[\frac{h}{\lambda}\right]^1+O\left[\left[\frac{h}{\lambda}\right]^2\right]\right\}\\&-\lambda^2\left[\frac{h}{\lambda}\right]^1[\tfrac{1}{3}-\tfrac{1}{15}\langle\omega^2\rangle\lambda^2+O(\lambda^4)]-\tfrac{1}{2}\lambda^4\left[\frac{h}{\lambda}\right]^2[-\tfrac{2}{15}\langle\omega\rangle+O(\lambda^2)]+O\left[\lambda^4\left[\frac{h}{\lambda}\right]^3\right]\ ,\end{aligned} \tag{E6b}$$

and where the variables, $h$, $\lambda$, and $t$ are related to $\sigma$, $H$, and $T$ via Eqs. (C1), (C2), and (E5), respectively. Of course, we have explicitly written only a few terms of the pertinent series, but higher-order terms, if needed, can easily be included using the mentioned expansions.


[1]T. Holstein and H. Primakoff, Phys. Rev. **58**, 1098 (1940).

[2]M. E. Fisher, in *Critical Phenomena,* edited by F. J. Hahne (Springer-Verlag, Berlin, 1983).

[3]N. N. Bogolyubov and S. V. Tyablikov, Dokl. Akad. Nauk SSSR **126**, 53 (1959).

[4]S. V. Tyablikov, *Methods of the Quantum Theory of Magnetism* (Nauka, Moscow, 1975).

[5]N. M. Plakida, *Some Problems of the Quantum Theory of Solids* (Moskovski Gosudarstvennyi Universitet, Moscow, 1974).

[6]B. Callen, Phys. Rev. **130**, 890 (1963).

[7]S. Katsura and T. Horiguchi, J. Phys. Jpn. **25**, 60 (1968).
[8]A. Kumar and A. Gupta, Phys. Rev. B **7**, 3968 (1983).
[9]J. Schreiber, Physica **96B**, 27 (1979).
[10]F. J. Dyson, Phys. Rev. **102**, 1217 (1956).
[11]L. Flax, Phys. Rev. B **5**, 997 (1972).
[12]D. J. Thouless, P. W. Anderson, and R. G. Palmer, Philos. Mag. **35**, 593 (1977).
[13]J. C. Le Guillou and J. Zinn-Justin, Phys. Rev. Lett. **39**, 95 (1977).
[14]T. H. Berlin and M. Kac, Phys. Rev. **86**, 821 (1952).
[15]*Magnetic Properties of Metals,* Vol. 19a of *Landolt-Börnstein Tables, New Series III,* edited by H.P.J. Wijn (Springer-Verlag, Berlin, 1986).
[16]E. Carre and J. Souletie, J. Magn. Magn. Mater. **72**, 29 (1988).
[17]P. Weiss and R. Forrer, Ann. Phys. (Paris) **5**, 153 (1926).
[18]J. S. Kouvel and B. J. Comly, Phys. Rev. Lett. **20**, 1237 (1968).
[19]I. S. Gradshtein and I. M. Rhyzhik, *Tables of Integrals, Series and Products* (Academic, New York, 1965).
[20]*Higher Transcedental Functions,* edited by A. Erdelyi (McGraw-Hill, New York, 1953), Vol. I.
[21]Kishin Mooriani and J. M. D. Coey, *Magnetic Glasses* (Elsevier, Amsterdam, 1984).
[22]G. Leibfried and N. Breuer, *Point Defects in Metals* (Springer-Verlag, Berlin, 1978).